

# 1 **Moisture Buffering in Buildings: A Review of Experimental and Numerical** 2 **Methods**

3 *Brenton K. Kreiger<sup>a</sup> and Wil V. Srubar III<sup>a†</sup>*

4 <sup>a</sup> Department of Civil, Environmental, and Architectural Engineering, University of Colorado Boulder,  
5 ECOT 441 UCB 428, Boulder, Colorado 80309-0428 USA, <sup>†</sup>Corresponding Author, T +1 303 492 2621,  
6 F +1 303 492 7317, E [wsrubar@colorado.edu](mailto:wsrubar@colorado.edu)

## 7 8 **Abstract**

9 The moisture buffering capacity in buildings is well known to influence material durability, building-  
10 scale energy efficiency, and indoor environmental quality. In this work, we present a comprehensive  
11 meta-analysis of experimental studies and a review of numerical approaches concerning the moisture  
12 buffering capacity of common building materials. More specifically, we synthesize and analyze reported  
13 moisture buffering values (MBVs) of materials from >180 unique characterization experiments. In  
14 addition, we classify, compare, and critically discuss experimental methods employed to measure MBV,  
15 along with numerical methods that have been used to quantify building-scale benefits. Experimental data  
16 indicate that biotic and chemically hydrophilic (*e.g.*, cellulosic) materials exhibit higher MBVs than  
17 porous, abiotic (*e.g.*, cementitious) materials, which suggests new opportunities for engineering natural,  
18 synthetic, and/or hybrid hydrophilic materials that display hyperactive MBVs. In addition, moisture  
19 buffering effects have been shown to yield up to 30% energy savings in certain climates. However, our  
20 analysis reveals that more consistent experimental and numerical methodologies are still needed to  
21 accurately quantify building-scale benefits. To this end, we identify specific gaps in scientific and  
22 technical knowledge and offer suggestions for experimental and theoretical research that is required to  
23 advance the collective understanding of moisture buffering and its effects on the energy consumption and  
24 indoor environmental quality of residential and commercial buildings.

25

26 **Keywords:** Moisture buffering, building materials, energy efficiency, indoor environmental quality.

## 27 **1.0 Introduction**

28 Active moisture management in residential and commercial buildings is an energy-intensive process. In  
29 2017, the United States (US) Energy Information Administration reported that building energy comprised  
30 39% of total US energy consumption [1], of which 92% was attributable to residential and commercial  
31 building heating, ventilation, and air-conditioning (HVAC) systems alone [1,2]. To maintain indoor  
32 environmental comfort, mechanically driven HVAC systems stabilize indoor relative humidity (RH)  
33 within specific ranges. In humid climates, for example, dehumidification requires both cooling and  
34 reheating air. Buildings with high indoor humidity (*e.g.*, natatoriums) require high degree of ventilation  
35 with conditioned air. Dehumidification, ventilation, and conditioning (*i.e.*, heating and cooling) are all  
36 energy-intensive processes that are required, in large part, to manage moisture in buildings.

37 Recent research shows that failing to account for passive moisture absorption and desorption of  
38 building materials during building operation can result in up to 210% overestimation of peak heating  
39 loads and 59% underestimation of heat flux from latent heat and moisture effects [3]. Over- and  
40 underestimations of these magnitudes can lead to the overdesign of HVAC systems in residential and  
41 commercial buildings because simulated energy consumption will increase due to increases in thermal  
42 conductivity of wall assemblies. Accounting for hygroscopic effects of spruce plywood, for instance, has  
43 been shown to yield up to 20-30% energy savings in terms of cooling loads in residential buildings [4–6].  
44 HVAC control strategies that consider passive moisture buffering of building materials have been shown  
45 to decrease energy consumption by 14-17% during heating periods [7]. In short, the passive ability of  
46 materials to absorb and desorb moisture is important to consider in estimating the peak heating and  
47 cooling demands in both residential and commercial buildings.

### 48 **1.1 Sources of Moisture in Buildings**

49 Moisture in buildings originates from several sources, including outdoor air and indoor plants, occupants,  
50 and release from high-water-content building materials (*e.g.*, wood, concrete) soon after construction. The  
51 moisture content of outdoor air depends heavily on climate zone, which dictates average RH, types and  
52 levels of precipitation (*e.g.*, snow, rain), and ground-level moisture. Indoor moisture conditions depend on

53 the type and amount of flora, as well as occupancy levels and associated activities. Humans can generate  
54 115 to 270 grams of water per hour (2.8 to 6.5 kg per day) through respiration and perspiration [8]. Water  
55 fixtures (*e.g.*, showers, sinks, toilets) and the evapotranspiration of indoor plants also significantly  
56 contribute to indoor moisture levels [8]. High-water-content construction materials will acclimate over  
57 time and release moisture into the building. Overall estimates for moisture released in the first year of  
58 new construction is ~10 kg per day [9]. More specifically, dimensional lumber utilized at a standard  
59 moisture content (*i.e.*, 15% or 19%) can release ~200 kg of water in an average residential single-family  
60 home as it equilibrates [9]. Concrete can release ~90 kg/m<sup>3</sup> over two years post-construction [9].  
61 Together, these outdoor and indoor sources of moisture impart non-trivial material, energy, and human  
62 health consequences in buildings, which are further discussed in the following sections [6].

63

## 64 **1.2 Building Health**

65 Moisture can trigger physical, mechanical, chemical, and biological deterioration mechanisms in building  
66 materials that can lead to building-scale damage. This has been a well-known problem for many years, in  
67 fact, previous research from over 40 years prior has reported that up to 90% of all construction material  
68 and building durability issues are caused by moisture [10]. Specifically, moisture content of hygroscopic  
69 structural materials, like wood, affects size (*e.g.*, swelling, shrinkage), strength, and stiffness [11]. Wu *et*  
70 *al.* [12] found that commercially available oriented strand board (OSB) exhibited 31% dimensional  
71 swelling with an increase in moisture content of 24%. In terms of mechanical properties, high moisture  
72 levels can result in up to 70% loss in allowable strength for wood members [13]. These physical and  
73 mechanical effects in wood can be exacerbated by moisture absorption and desorption cycling [14].  
74 Moisture can also lead to other physical, mechanical, and chemical deterioration effects, such as  
75 efflorescence [15], hydrolytic and exacerbated UV degradation of polymeric materials [16], chloride-  
76 induced corrosion in reinforced concrete [17], and freeze-thaw deterioration [18]. Regarding biological  
77 deterioration, moisture can induce localized conditions for mold and fungal growth, which can accelerate  
78 material aging [19]. RH is intimately related to mold growth rates, where mold growth depends on the

79 frequency of low and high humidity levels and time of wetness [19]. In a 2001 study led by Klaus  
80 Sedlbauer, 250 sources were reviewed to establish mold growth isopleths on common building materials  
81 [20]. The LIM (Lowest Isopleth for Mold) begins at 75% RH with up to 2 mm/day of growth at 85% RH  
82 and 5 mm/day above 95% RH [20]. Biological deterioration is of critical concern regarding not only the  
83 structural integrity of biotic materials (*e.g.*, wood), but also the potential negative effects on indoor  
84 environmental quality and associated consequences to human health and well-being.

### 85 **1.3 Human Health**

86 Both high and low levels of moisture in indoor air have been linked to health problems since the early  
87 20th century. In seminal studies, researchers linked dry air from furnace-heated homes in a New England  
88 winter to skin and respiratory irritation [21] and to the diminishing health of children in grammar schools  
89 [22]. In the 1910s, researchers showed that 40% RH in residential buildings of the era was enough for  
90 condensation—and the health-related problems that follow—to occur [23]. Recent research has shown  
91 that conditioned air with RH >40% relieves nasal, pharyngeal, and skin dryness and congestion [24].  
92 While low RH causes adverse health effects, excess RH, has also been linked to other respiratory  
93 illnesses, such as asthma, wheezing, and bronchial hyper-responsiveness (BHR) [25]. Additionally, high  
94 humidity levels can cause occupant discomfort and can alter the perception of indoor air quality [26]. In  
95 other words, humans will perceive humid indoor air as heavy, muggy, and uncomfortable and less  
96 sanitary to breath. Given that humans spend an average of 90% of their time indoors (*e.g.*, homes, offices,  
97 schools) [27] and that high (>70%) or low (<40%) RH imparts measurable health effects [28], confining  
98 RH levels to prescribed, acceptable ranges is of critical importance in building operations.

### 99 **1.4 Impact and Scope of Review**

100 Moisture buffering as a passive humidity regulation strategy is both an economical and energy-efficient  
101 approach that is currently not fully understood and, consequently, underexploited in building design and  
102 construction. This review critically explores the experimental and numerical methods of quantifying  
103 moisture buffering effects and estimating their building-scale impact. First, experimental methods  
104 employed to measure moisture buffering values (MBVs) of building materials are classified, compared,

105 and reviewed. Empirical MBV data from >180 characterization experiments are synthesized and analyzed  
106 to elucidate the physical, chemical, and biological characteristics of materials that display particularly  
107 high MBVs. Second, hygrothermal modeling methods for building-scale applications are classified and  
108 critically analyzed based on computational expense, convenience, and accuracy. Finally, new, emerging  
109 research on the moisture buffering properties of innovative hygroscopic materials is highlighted. We  
110 conclude this review by discussing new opportunities and future research directions that are required to  
111 advance technical understanding, material development, and computational modeling of moisture  
112 buffering effects and to leverage the benefits in the design, construction, and operation of residential and  
113 commercial buildings.

114

## 115 **2.0 Review of Experimental Methods**

### 116 **2.1 Characterization Methods**

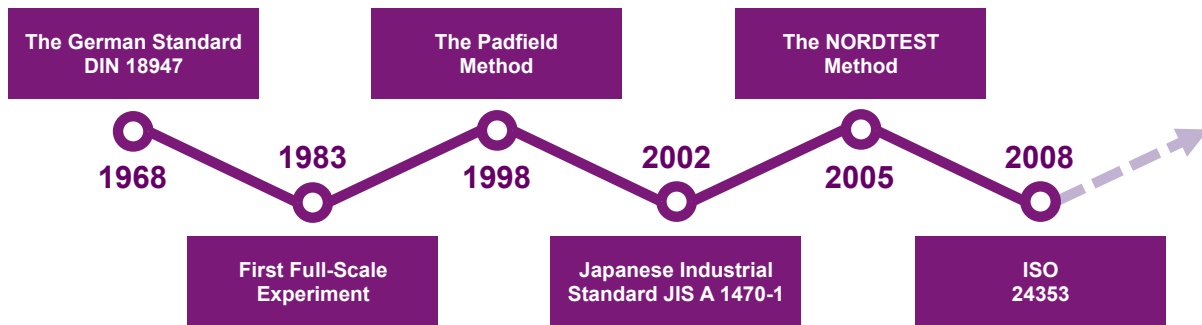
117 Moisture buffering value (MBV) is the most well accepted parameter that is used to describe and compare  
118 the moisture buffering capacities of different building materials. MBV, defined as the change in mass per  
119 square meter per change in RH ( $\text{g}/\Delta\text{RH}/\text{m}^2$ ), is most commonly characterized by a stepwise vapor  
120 sorption process—a method that involves a measurement of mass change with discrete increases or  
121 decreases in RH over various time steps. MBV is calculated according to the following [29,30]:

$$122 \quad MBV = \frac{G}{\Delta RH} \quad (\text{Equation 2.1})$$

123 where G is the moisture uptake in  $\text{g}/\text{m}^2$  throughout a prescribed RH cycle.

124 **Figure 1** illustrates the historical evolution of MBV characterization methods. Seminal moisture  
125 buffering capacity research was conducted in Germany at the Fraunhofer Institute of Building Physics and  
126 at Lund University in Sweden in the late 1960s. By developing the step-response method that is still used  
127 to characterize moisture sorption in response to cyclic, time-dependent changes in RH [31], these  
128 experiments set the standard for contemporary moisture buffering experimentation. Following these  
129 studies, the Padfield method was developed as an alternative to the stepwise model [32]. The Padfield

130 method draws an analogy to thermal capacitance by defining the moisture capacitance of air using the unit  
131 of *buf*, which cannot be compared to the more standard MBV unit of  $g/\Delta RH/m^2$ . The *buf* is reported in  
132 meters and refers to the height of  $1\text{ m}^2$  column of air. The higher the moisture capacitance of a material,  
133 the higher the *buf* and the greater effective volume of air that can hold moisture. The Padfield method is  
134 distinct in that it does not define MBV as an intrinsic material property. The most recent methods that  
135 have been developed, including the Japanese Industrial Standard [33], NORDTEST [29], and ISO[34]  
136 methods, however, have all used stepwise RH variation as a primary approach to characterize MBV.  
137



138  
139 **Figure 1.** Historical milestones in experimental methods for MBV.

## 140 141 **2.2 Material- and Building-Scale Experimental Methods for Evaluating MBV**

### 142 2.2.1 *The German Standard DIN 18947*

143 The German-developed standard *DIN 18947* [35], which was developed specifically for characterizing the  
144 hygric properties of earthen plasters, is the oldest standard using methods first proposed in 1965 by  
145 Kunzel. The prescribed method applies cyclic conditioning of RH between 50% and 80% in 12 hour  
146 cycles. Percent-mass changes over that prescribed RH range is used to define moisture buffering capacity.  
147 The original German standard has not been widely applied and cited in the literature, as only two of the  
148 188 published experimental tests reviewed in this work employed *DIN 18947*. However, additional  
149 references that were reviewed indicate that this standard has been most often used internally by German  
150 industry researchers to characterize and compare hygric performances of different materials [36–38]].

151 2.2.2 *The Padfield Method*

152 The Padfield Method, developed by Tim Padfield in 1998, specifically focused on moisture buffering  
153 capacity of materials as it relates to historic preservation of buildings [32]. The method prescribes a small,  
154 cyclic step-response procedure between 50% and 60% RH. The aim of this method—and what  
155 differentiates it from others—is that it quantifies the effect of hygroscopic materials on ambient RH as  
156 opposed to the opposite, standard measurement, which quantifies the effect of cyclic RH on changes to  
157 material mass. The basic experimental set-up consists of a sealed chamber with a water reservoir and  
158 controlled air speed that varies between 0.2-1.2 m/s to ensure adequate mixing. The temperature of the  
159 water, adjusted by a thermoelectric heat pump, controls the RH of the sealed chamber. The method  
160 assumes that all water lost from the reservoir is absorbed by the test material. While a benefit of this set-  
161 up is that any geometry of sample can be tested, one drawback is the water sorption of equipment and air  
162 must be corrected in the quantitative analysis to ensure accurate results. As previously discussed, the unit  
163 to report moisture buffering was defined as the *buf* in the Padfield method, which cannot be directly  
164 compared to MBV [32].

165 2.2.3 *Japanese Industrial Standard JIS A 1470-1*

166 Introduced in 2002, the Japanese Industrial Standard (JIS A 1470-1) [33] employs a similar step-response  
167 method established by the German Standard DIN 18947. The experimental procedure involves a stepwise  
168 preconditioning method that first equilibrates materials at 23 °C and at either 43%, 63%, or 83% RH,  
169 prior to a stepwise dynamic conditioning procedure. A minimum sample area of 100 cm<sup>2</sup> is required.  
170 Most studies utilize rectangular prism geometries in which all sides except one are sealed with aluminum  
171 tape to effectively capture the effects of 1D moisture transport. While similar to the DIN 19847 standard  
172 and other methods that followed its development (*e.g.*, NORDTEST), the JIS method is unique. First,  
173 there is an equal stepwise cyclic conditioning procedure that involves cycles of 24 hours of high humidity  
174 exposure and 24 hours of low humidity exposure. Three cyclic conditioning RH levels are specified: 33%  
175 to 53%, 53% to 75%, and 75% to 93% RH. Second, the material surface film resistance (a function of air  
176 speed around and geometry of sample) is prescribed as  $4.80 \pm 0.48 \times 10^7$  Pa/kg. Third, the material

177 thickness must be equal to the actual, realistic thickness of the product to be tested [38,39], since, as  
178 discussed, material thickness can make a significant impact on moisture buffering value [40]. Overall,  
179 while this is an established and accepted method, none of the published studies in this review utilized the  
180 JIS procedure, as it is not usually referred to in English publications [38].

#### 181 2.2.4 *The NORDTEST Method*

182 Since 2005, the NORDTEST Method has been the most popular standard for hygroscopic characterization  
183 of materials. The procedure was developed to create a standardized test method that characterized a well-  
184 definable and consistent material property. The NORDTEST method established the conventional  
185 definition of MBV as it is referred to herein and defined broad categories of MBV from negligible to  
186 excellent for commercial comparison of materials (see **Table 1**). During its development, university  
187 researchers carried out round-robin MBV tests to evaluate the consistency of experimental protocol across  
188 material types. Because results from the round robin tests among universities showed good agreement, the  
189 high repeatability and consistency of results propelled the popularity of the NORDTEST method.

190 Over 70% of the studies reported herein used an official or modified version of the NORDTEST  
191 method. The experimental method consists of a 24-hour cyclic RH stepwise variation between 33% RH  
192 for 16 hours and 75% RH for 8 hours. A common modification of the NORDTEST method, the *two-*  
193 *bottle method*, was used in research facilities that could not meet the NORDTEST chamber conditioning  
194 criteria but used similar principles with slightly different RH values between 50% and 80%. Similar to the  
195 JIS method, samples tested using the NORDTEST method must be a minimum of 100 cm<sup>2</sup> of rectangular  
196 geometry. However, where the JIS method specifies that the thickness of the sample must be the thickness  
197 of the product, the NORDTEST method only states that the sample must have a thickness greater than the  
198 calculated theoretical moisture penetration depth (TMPD). This requirement is important, because a study  
199 by Roels and Janssen [39] demonstrated through a sensitivity analysis that the main reason for difference  
200 in MBV values between JIS and NORDTEST method testing of samples was the sample thickness. For  
201 exposure to RH, samples are covered on all but one or two sides with aluminum tape to ensure realistic  
202 conditions of exposure to indoor air [29,38]. If two sides are left exposed, the calculated MBV must be



203 divided by two. Samples are generally pre-conditioned at 23 °C and 50% RH until hygroscopic  
204 equilibrium by weight is achieved, prior to the test. As mentioned above, the experiment involves cyclic  
205 RH variation, which can be achieved using a climate chamber or with salt solutions in sealed chambers.  
206 Temperature is held isothermally at 23 °C. As a criterion to stop the test, the NORDTEST and most other  
207 methods require a quasi-steady-state equilibrium to be reached in which the change in mass between  
208 absorption and desorption steps varies less than a pre-defined threshold [41], since the slope of initial  
209 moisture intake is shown to overestimate actual MBV [41]. Additionally, while the NORDTEST method  
210 does not specify any ventilation rate for testing, the standard does mention an important inverse  
211 relationship between ventilation and MBV and states that the sample surface air speed should be  $0.10 \pm$   
212  $0.05$  m/s, which corresponds to a surface film resistance of  $5.0 \times 10^7$  m<sup>2</sup>-s-Pa/kg [42]. The difference  
213 between this value and the  $4.8 \times 10^7 \pm 10\%$  m<sup>2</sup>sPa/kg value set forth in the JIS method is important  
214 because of the established inverse relationship between surface film resistance and MBV.

215

216 **Table 1.** MBV classification system established by the NORDTEST method [29].

| MBV Class  | Minimum Level   | Maximum Level |
|------------|---|---------------|
|            | MBV (g/ΔRH/m <sup>2</sup> )<br>8 hours @ 75% RH and 16 h @ 33% RH |               |
| Negligible | 0   | 0.2           |
| Limited    | 0.2   | 0.5           |
| Moderate   | 0.5   | 1.0           |
| Good       | 1.0   | 2.0           |
| Excellent  | 2.0   | >2.0          |

217

### 218 2.2.5 ISO 24353

219 The first edition of ISO 24353 [34] was published in 2008 and is based on the JIS method. Similar to the  
220 JIS method, samples are prepared with aluminum tape sealing all of the sides except one and must have a  
221 minimum surface area of 100 cm<sup>2</sup>. Preconditioning occurs at 23 °C and either 43%, 63%, or 83% RH, and

222 step cycles occur over 12 hour periods from 33%-53%, 53%-75%, and 75% -93%. Similar to the JIS,  
223 there is no specified method for maintaining RH values, unlike the NORDTEST method that requires a  
224 climate chamber or salt solutions. However, these are proven to be the most cost effective and simple  
225 experimental setups and used consistently in studies that employ the ISO standard [38]. Given its  
226 relatively recent establishment, this method has been rarely utilized and, therefore, scarcely cited in the  
227 published studies considered in this review.

#### 228 2.2.6 Ultimate Moisture Buffering Value (UMBV)

229 UMBV is an adaptation of the NORDTEST MBV [43] that accounts for adverse temperature and  
230 humidity conditions that are more representative of four-season climate zones. The high humidity level  
231 corresponds to 98% and the low corresponds to 3% with temperatures ranging from 18 to 40 °C. Samples  
232 are preconditioned at a standard 23 °C and 50% RH until hygroscopic equilibrium is achieved. Using  
233 these parameters, the MBV is calculated and multiplied by a time coefficient,  $\alpha$ , determined by the rough  
234 frequency of exposure to these conditions in four seasons:

$$235 \quad UMBV = \sum_{i=1}^{III} \alpha_i MBV_i \quad (\text{Equation 2.2})$$

236 where  $\alpha$  is the time coefficient, or total hr/day each sample is subjected to the specified RH. The  $\alpha$   
237 parameter is simply calculated by  $t/24$  where  $t$  varies based on the stage of the UMBV test (see **Table 2**).  
238 The resulting equation computes the comprehensive moisture tolerance of the material over three stages  
239 that correspond to damp-proofing capability, adsorption, desorption, and instantaneous response capacity,  
240 as illustrated in the table below.

241

242 **Table 2.** Summary of UMBV testing conditions.

| Stage | Temperature (C) | RH (%)       | Time (hr/day) | Practical Application                          |
|-------|-----------------|--------------|---------------|--|
| I     | $23 \pm 0.3$    | $50 \pm 0.3$ | 12            | Damp-proofing, instantaneous response capacity |
| II    | $40 \pm 0.3$    | $98 \pm 0.3$ | 8             | Damp-proofing, adsorption                      |

|     |              |             |   |   |
|-----|--------------|-------------|---|---|
| III | $18 \pm 0.3$ | $3 \pm 0.3$ | 4 | Desorption, instantaneous response capacity |
|-----|--------------|-------------|---|---|

243 2.2.7 Full-Scale Experimentation

244 Despite advances in material-scale characterization, full-scale experimentation is arguably a more  
245 accurate method to gather experimental data on moisture buffering capacity or to validate predictive  
246 models that quantify energy and environmental benefits of moisture buffering. Intuitively, however, full-  
247 scale experiments are more expensive, time-consuming, and rarely reported in the literature. Additionally,  
248 completely non-hygroscopic houses do not necessarily exist due to the hygroscopic nature of furnishings  
249 and other coating materials [44]. Some full-scale experiments were performed in Holzkirchen, Germany,  
250 in which researchers used a large climate chamber to show that moisture buffering capacity of gypsum  
251 board could reduce peak humidity up to 44% [31]. Fraunhofer-Institute of Building Physics in  
252 Holzkirchen conducted another similar experiment to validate the widely used WUFI software, in which  
253 the moisture buffering effects of a reference room covered in aluminum was compared to that a wood-  
254 clad test room [45]. Using tracer gases to track ventilation rates and exposed hygroscopic surface area to  
255 measure moisture transfer, a test house in Helsinki, Finland, compared a wood-framed home with and  
256 without a polyethylene vapor retarder to show 15% RH peak reductions at 27° C, also concluding that  
257 material moisture buffering is more effective than increasing ventilation rates from 0.08 to 0.55 ACH  
258 [46]. More recently, Shi *et al.* conducted a full-scale experiment to test non-standard building materials by  
259 outfitting a typical civil defense shelter in Beijing for field measurements and numerical validation [2].  
260 Allinson and Hall [38] monitored the interior moisture buffering effect of a rammed earth shed. Huibo  
261 Zhang *et al.* [45] conducted a moisture buffering experiment under real-world conditions. In a study by  
262 Luyang Shi *et al.*, two rooms were set-up within a real home in order to compare a test room to a  
263 reference point to evaluate porous ceramic tile, biomass fiber wallpaper, and vermiculite board [46].  
264 Overall, full-scale implementation is a comprehensive practice for eliminating major assumptions and  
265 gathering realistic data on the applied moisture buffering effect of a building assembly. However, the  
266 drawbacks for space, time, and cost, are significant, which has motivated the industry to develop *in-situ*

267 characterization practices through numerical modeling and material-scale experimentation to define MBV  
268 as a material property.

### 269 **2.3 Characterization Methods: Key Assumptions**

270 In addition to employing different experimental approaches to characterize and report MBV, each method  
271 makes key assumptions that affect the general applicability of material-scale MBV to building-scale  
272 behavior. As discussed in the next section, very few studies go as far as to experimentally measure the  
273 moisture buffering effect of materials within building systems [31,38,45,47,48], and no studies that were  
274 reviewed experimentally report building-scale application of highly absorbing materials. However, many  
275 numerical studies have relied on material-scale characterization of MBV to estimate the effect of moisture  
276 buffering on building energy consumption, thus placing high dependence on the MBV experimental  
277 methods to adequately capture moisture buffering capacity of different building materials.

278         The primary assumptions inherent to a majority of MBV experimental methods—and their  
279 potential consequences in terms of building-scale applicability of MBVs obtained by these methods—are  
280 as follows:

- 281 1. *Stepwise changes in RH are representative of RH changes in indoor environments.* The potential  
282 energy savings of moisture buffering come from the ability of materials to passively dampen RH  
283 peaks. Hygroscopic materials interact dynamically with indoor RH rather than discretely, as assumed  
284 by the stepwise methodology. Therefore, given that RH will vary continuously with moisture content  
285 of indoor surface materials and not remain constant for a period of time [49], providing a constantly  
286 high or low RH environment to test a material may overestimate the MBV.
- 287 2. *The method parameters for number of cycles, temperature, and RH sufficiently provide conditions in*  
288 *which equilibrium can be achieved for all materials.* Test methods specify isothermal conditions,  
289 relevant RH steps, and a tolerance for mass variations, representative of quasi-steady state  
290 equilibrium. However, this does not directly relate to building applications because the material is not  
291 always responding with a MBV corresponding to its quasi-equilibrium state. This assumption is

292 important, because absorption and desorption can differ—and the calculation of overall MBV can  
293 differ – from equilibrium values [29].

294 3. *Sample thickness is larger than its theoretical moisture penetration depth (TMPD)*. Theoretical  
295 moisture penetration depth is defined as the point at which moisture content variations are only 1% of  
296 those on the surface [29]. Most experiments assume that the TMPD is within the sample thickness  
297 without substantiating it being so. A study by M. Rahim *et al.* [40], however, illustrated that MBV  
298 continued to increase  $0.3 \text{ g}/\Delta\text{RH}/\text{m}^2$  when varying the sample thickness from 3 to 7 cm while TMPD  
299 was previously calculated at 3.14 cm. This finding indicates that MBV may continue to increase with  
300 thickness, regardless of TMPD.

301 4. *Moisture diffusivity remains constant throughout testing*. Studies assume moisture diffusivity remains  
302 constant within the RH range of 30% to 70%, which is approximately within the bounds used in most  
303 MBV studies and realistic conditions for building applications. However, moisture diffusivity is well  
304 known to be concentration-dependent [50], and the chemistry of different materials can dictate single  
305 or multiple mechanisms of moisture transport (*e.g.*, diffusion, sorption, permeation) [50], which will  
306 affect the concentration-dependence of its diffusivity. Therefore, given the wide range of responses of  
307 materials to moisture, the static diffusivity assumption imparts unknown variability in the definition  
308 of MBV as an inherent material property. Deviations beyond the RH range of 30-70% have also been  
309 shown to exhibit significant variations in moisture diffusivity depending on RH [51].

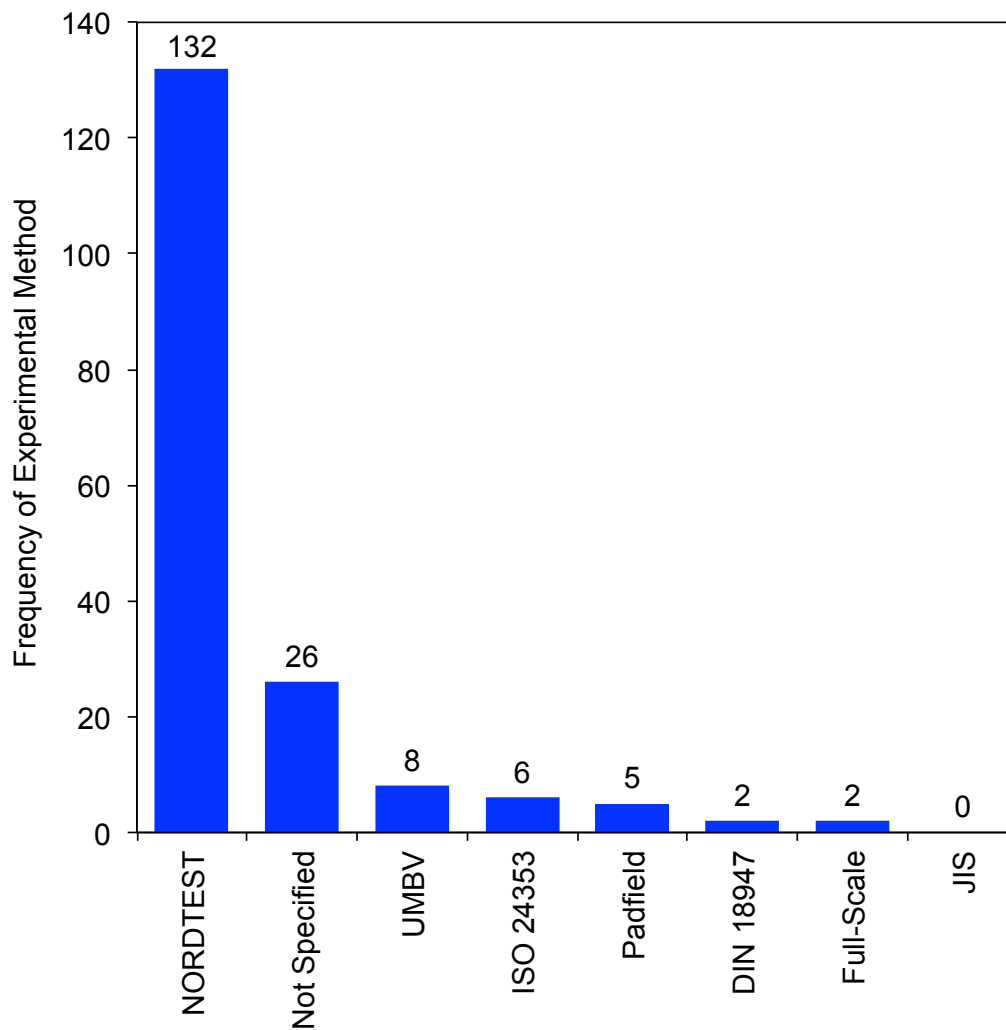
310 5. *Ventilation and airflow across the sample is negligible*. Ventilation is mentioned in various standards  
311 (*e.g.* JIS, NORDTEST), yet not considered homogenously across many studies. For example, Colinart  
312 *et al.* [50] and Nguyen *et al.* [51] do not mention the effect of airflow in their testing of hemp  
313 concrete and bamboo fibers. However, air flow will affect localizes surface RH. The MBV review of  
314 earthen materials by Svennberg *et al.* [31] states that lower air change per hour (ACH) rates will yield  
315 higher RH levels, which can inevitably affect the definition of MBV by up to 20%. Shi *et al.* [47]  
316 confirmed this by measuring ACH with tracer gases to test the effect of five different ventilation rates  
317 on MBV and confirmed that they have a significant impact on measured MBV. These findings not

318 only illustrates the importance of holding ventilation rate constant in determining MBV, but also  
319 suggests that differing ventilation rates in real building applications may account for the  
320 inconsistencies between material-scale MBV measurements and building-scale moisture buffering  
321 behavior.

## 322 **2.4 Meta-Analysis of Experimental Data**

### 323 *2.4.1 MBV Method Frequency*

324 Despite the wide variety of methods previously described, the NORDTEST method remains the most  
325 widely applied—and, therefore, the most comparable—method to characterize moisture buffering  
326 capacities of building materials. **Figure 2** illustrates the frequency of different methods applied in the  
327 studies reviewed herein. As shown in **Figure 2**, the NORDTEST method was most frequently employed  
328 (>70% of studies) to measure MBV, while methods “Not Specified” and the UMBV method were the  
329 second and third most commonly applied, respectively. Only five studies employed the Padfield Method,  
330 which, as discussed, does not utilize the conventional step-response procedure prescribed by the other  
331 methods.



332

333

**Figure 2.** Frequency of methods used to experimentally determine MBV.

334

#### *2.4.2 MBV Experimental Data*

335

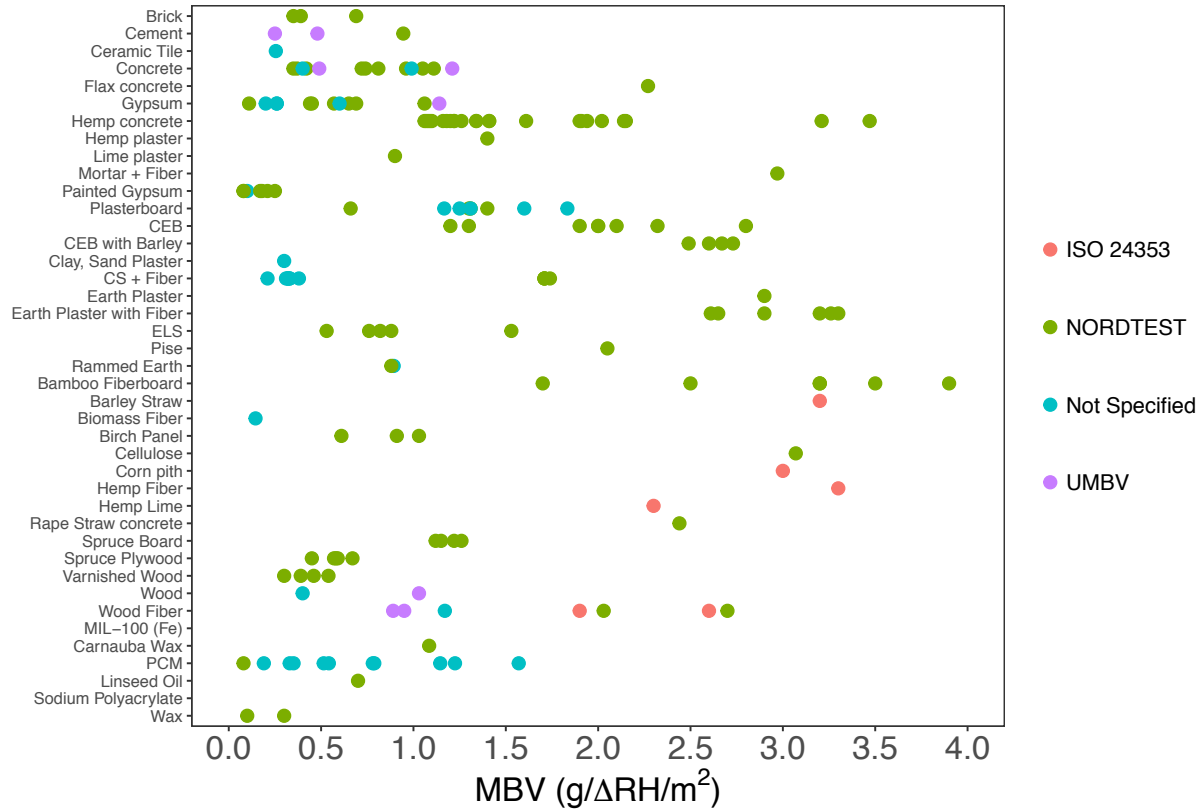
A comprehensive visualization of reported MBVs is shown in **Figure 3**. This chart illustrates how widely

336

MBV varies across individual studies and measurement methods, as well as variation within identical

337

materials and between different materials.



338

339 **Figure 3.** Reported MBV of building materials. CEB = compressed earth block, CS = clay-sand, ELS =  
 340 engineered local soil, PCM = phase change material [29,30,55–64,40,65–69,42,43,47,48,52–54].

341

342 **Table 3** reports statistical data for reported MBV, density, porosity, and the method by which MBV  
 343 was characterized per material reviewed herein. We report different MBVs in **Table 3** for materials that  
 344 were characterized by different methods.

345



346 **Table 3.** Statistical summary of reported MBV, porosity, and density by material and method. CEB =  
 347 compressed earth block, CS = clay-sand, ELS = engineered local soil, PCM = phase change material.  
 348 Note that one standard deviation is used, representing a 67% confidence interval.

| Material              | n  | MBV                  |               | Porosity    | Density (kg/m <sup>3</sup> ) | References |
|-----------------------|----|----------------------|---------------|-------------|------------------------------|------------|
|                       |    | g/ARH/m <sup>2</sup> | Method        |             |                              |            |
| Bamboo Fiberboard     | 6  | 3.0 ± 0.79           | NORDTEST      | N/A         | 404 ± 85                     | [53]       |
| Barley Straw          | 1  | 3.2                  | ISO 24353     | 92%         | 108                          | [55]       |
| Birch Panel           | 3  | 0.85 ± 0.22          | NORDTEST      | N/A         | 600                          | [29]       |
| Brick                 | 3  | 0.48 ± 0.19          | NORDTEST      | N/A         | 1600                         | [29]       |
| Carnauba Wax          | 1  | 1.1                  | NORDTEST      | N/A         | N/A                          | [58]       |
| CEB                   | 7  | 1.9 ± 0.54           | NORDTEST      | N/A         | 1800                         | [63]       |
| CEB + Barley Straw    | 4  | 2.6 ± 0.10           | NORDTEST      | N/A         | 1735 ± 71                    | [55]       |
| Cellulose             | 1  | 3.1                  | NORDTEST      | N/A         | N/A                          | [59]       |
| Cement                | 2  | 0.37 ± 0.16          | UMBV          | N/A         | 1925 ± 153                   | [43]       |
| Ceramic               | 1  | 0.26                 | Not Specified | N/A         | 1740                         | [70]       |
|                       | 1  | 0.95                 | NORDTEST      | N/A         | 1500                         | [42]       |
| Clay Plaster + Fiber  | 4  | 1.7 ± 0.02           | NORDTEST      | 41 ± 2.8%   | 1544 ± 144                   | [67]       |
| Clay, Sand Plaster    | 9  | 0.31 ± 0.05          | Not Specified | N/A         | N/A                          | [56]       |
|                       | 2  | 0.85 ± 0.51          | UMBV          | N/A         | 1346 ± 1279                  | [43]       |
|                       | 2  | 0.70 ± 0.42          | Not Specified | N/A         | N/A                          | [71]       |
| Concrete              | 10 | 0.88 ± 0.56          | NORDTEST      | 70.6%       | 1335 ± 762                   | [29,30]    |
|                       | 1  | 3.0                  | ISO 24353     | 98%         | 48.1                         | [55]       |
| Earth Plaster         | 1  | 2.9                  | NORDTEST      | N/A         | 1848                         | [55]       |
| Earth Plaster + Fiber | 6  | 3.0 ± 0.31           | NORDTEST      | N/A         | 1362 ± 242                   | [55]       |
| ELS                   | 5  | 0.90 ± 0.37          | NORDTEST      | 22.3 ± 2.2% | 2076 ± 65                    | [69]       |
|                       | 1  | 0.15                 | Not Specified | N/A         | 300                          | [70]       |
|                       | 1  | 1.1                  | UMBV          | N/A         | 874                          | [43]       |
| Gypsum                | 4  | 0.33 ± 0.18          | Not Specified | N/A         | N/A                          | [56,61,71] |
|                       | 10 | 0.45 ± 0.30          | NORDTEST      | N/A         | 977 ± 204                    | [29,54,59] |
| Gypsum, Lime Plaster  | 3  | 0.14 ± 0.06          | NORDTEST      | N/A         | 900                          | [54]       |
| Hemp Concrete         | 7  | 1.89 ± 0.32          | NORDTEST      | 76.4 ± 2.7% | 713 ± 645.5                  | [30,52,64] |
| Hemp Fiber            | 1  | 3.3                  | ISO 24353     | 97%         | 41.1                         | [65]       |
| Hemp Lime             | 1  | 2.3                  | ISO 24353     | 83%         | 286                          | [65]       |
| Hemp Lime Assembly    | 19 | 1.5 ± 0.70           | NORDTEST      | N/A         | 610 ± 453                    | [62]       |
| Laminated Wood        | 3  | 0.46 ± 0.08          | NORDTEST      | N/A         | 430                          | [29]       |
| MIL-100 (Fe)          | 1  | 15                   | NORDTEST      | N/A         | N/A                          | [68]       |
| Mortar + Fiber        | 1  | 3.0                  | NORDTEST      | N/A         | N/A                          | [66]       |
| Painted Gypsum        | 1  | 0.33                 | Not Specified | N/A         | N/A                          | [56]       |
| PCM                   | 1  | 0.08                 | NORDTEST      | N/A         | N/A                          | [59]       |
|                       | 9  | 0.81 ± 0.43          | Not Specified | 80%         | 793 ± 351                    | [61,71]    |
| Pise                  | 1  | 2.1                  | NORDTEST      | 24.2%       | 1870                         | [57]       |
| Plaster               | 3  | 1.1 ± 0.40           | NORDTEST      | N/A         | 670                          | [62,63]    |
| Plywood               | 1  | 1.0                  | UMBV          | N/A         | N/A                          | [43]       |
| Rammed Earth          | 1  | 0.88                 | NORDTEST      | N/A         | 1980                         | [69]       |
| Rape Straw Concrete   | 1  | 2.4                  | NORDTEST      | 75.1%       | 1954                         | [30]       |
| Sand, Lime Plaster    | 1  | 0.90                 | NORDTEST      | N/A         | 1650                         | [52]       |
| Sodium Polyacrylate   | 1  | 9.0                  | NORDTEST      | N/A         | N/A                          | [59]       |
| Spruce Board          | 4  | 1.2 ± 0.06           | NORDTEST      | N/A         | 430                          | [29,58]    |
| Spruce Board (sealed) | 4  | 0.35 ± 0.25          | NORDTEST      | N/A         | N/A                          | [58]       |
| Spruce Plywood        | 5  | 0.57 ± 0.08          | NORDTEST      | N/A         | N/A                          | [29]       |
| Vermiculite Board     | 1  | 0.19                 | Not Specified | N/A         | 746                          | [48]       |
| WSE Mortar Assembly   | 2  | 0.92 ± 0.04          | UMBV          | N/A         | 637 ± 21                     | [43]       |
| Wood                  | 1  | 0.4                  | Not Specified | N/A         | N/A                          | [61]       |
| Wood Fiberboard       | 1  | 1.2                  | Not Specified | N/A         | N/A                          | [71]       |
|                       | 2  | 2.4 ± 0.47           | NORDTEST      | N/A         | 458 ± 4                      | [62]       |
| Wood Fiber            | 2  | 2.3 ± 0.50           | ISO 24353     | 91 ± 7.1%   | 136 ± 108                    | [65]       |

350 As evidenced by the data presented in **Figure 3** and **Table 3**, high variability exists for the reported  
351 values of MBV and other intrinsic material properties. Previous authors have noted that results from  
352 hygric experimentation can be significantly affected by differences in the experimental set-up and  
353 operator error, while the results can also be affected by other protocol and geometry factors, including  
354 number of cycles and sample size [72]. However, some error in results appears inherent to various testing  
355 methods regardless of corrections made for minor differences in the experimental set-up. For example,  
356 findings from a round robin test with 14 participating laboratories illustrate that sorption isotherm testing  
357 is consistent, yet vapor permeability procedures yield significantly different results across labs [73].

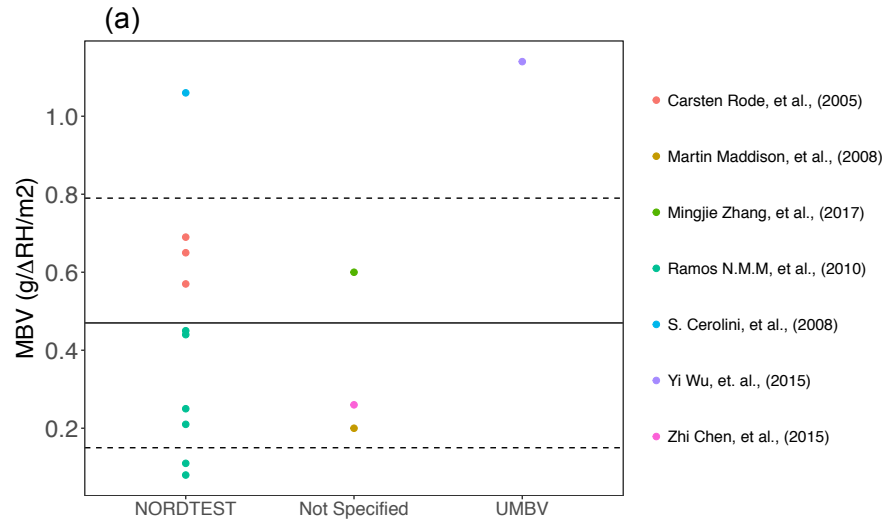
358 **Figure 4a-4c** highlights the high variability that can arise due to inconsistencies between methods,  
359 material heterogeneity, and operator error, respectively. **Figure 4a** depicts variability amongst MBV  
360 experimental methods, in which three major methods testing 13 different gypsum board samples were  
361 compared. The average across all studies was  $0.47 \pm 0.32 \text{ g}/\Delta\text{RH}/\text{m}^2$ , which represented the largest  
362 deviation amongst the three error sources compared. These results are expected because the *method error*  
363 also encapsulates *operator error* because seven different studies are compared and no data in which the  
364 lab used multiple studies to quantify MBV was available. However, using standard deviation for  
365 quantifying error, *method error* still significantly increases the variability of the test even when *operator*  
366 *error* is included.

367 **Figure 4b** depicts variability throughout a clay and sand plaster material measured multiple times  
368 in the same study [56] using the same testing method (in-house climate chamber) to remove any operator  
369 or method error. Sample variability resulted in the lowest error with an average of  $0.31 \pm 0.05 \text{ g}/\Delta\text{RH}/\text{m}^2$ .  
370 This finding illustrates that there will likely always been an inherent *material heterogeneity error* from  
371 physical variability, which can be accentuated by *operator error* and *method error*.

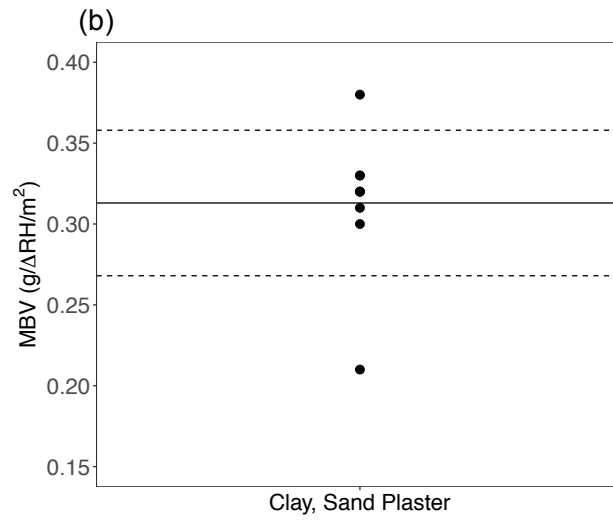
372 **Figure 4c** illustrates potential deviations from the mean caused by *operator error*, comparing  
373 various spruce board MBV studies from five different universities that all employed the NORDTEST  
374 method. The mean MBV obtained was  $0.57 \pm 0.08 \text{ g}/\Delta\text{RH}/\text{m}^2$  and ranged from 0.67 to  $0.45 \text{ g}/\Delta\text{RH}/\text{m}^2$ . In  
375 these examples, *operator error* is less significant than method consistency, yet more important in terms of

376 variability than *material heterogeneity*. These results agree with findings from previous sensitivity  
377 analyses on MBV error factors, which reported that *operator error* is the most significant source of error  
378 [72].  
379

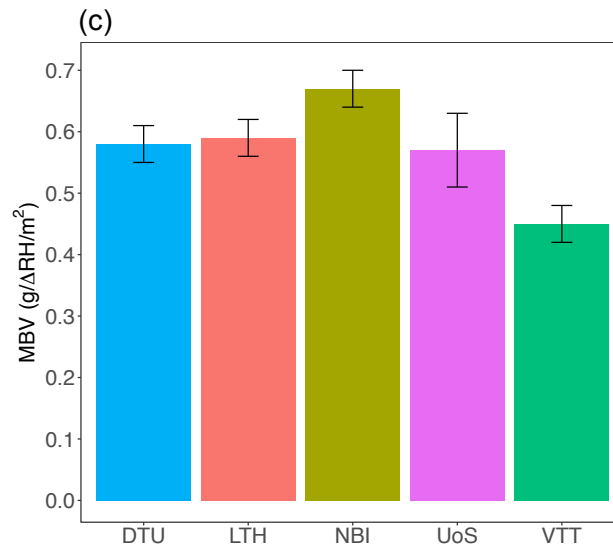
380



381  
382



383  
384



385

386 **Figure 4.** Variability imparted by **(a) Method:** Gypsum board characterization across different study  
387 methods. Dashed lines represent within one standard deviation of the mean (solid line); **(b) Material**  
388 **Heterogeneity:** Variability in MBV of different clay and sand plaster samples. Boundary lines represent  
389 one standard deviation of the mean (middle line); **(b) Operator Error:** Spruce Plywood characterization  
390 between different testing facilities.

391

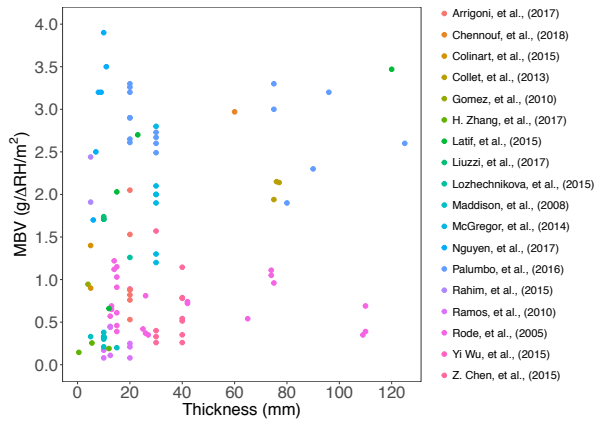
#### 392 *2.4.3 MBV vs. Thickness, Density, and Porosity*

393 The relationship between MBV and thickness, density, and porosity is graphically illustrated in **Figure**  
394 **5a**, **Figure 5b**, and **Figure 5c**, respectively. As shown in **Figure 5a**, sample thickness did not correlate  
395 well with reported MBV. This result was anticipated, given that thickness is an inherent physical property  
396 of each sample and directly relates to the total theoretical capacity of that sample to fully absorb moisture  
397 throughout the bulk, while MBV is an explicitly characterized surface-dominated capability of materials  
398 to passively buffer moisture in the air. A simple least-squares regression shows no relationship between  
399 thickness and MBV. This result is most likely due to the fact that most studies are based off of the  
400 NORDTEST method which requires a material sample thickness greater than its theoretical moisture  
401 penetration depth (TMPD) [29]. However, at least one study shows that moisture sorption capacity can  
402 display a linearly increasing relationship with thickness and MBV as thickness is increased past its TMPD  
403 [74]. While no argument is made for this correlation, it is hypothesized that moisture, once absorbed by  
404 the material, can move into the bulk *via* other transport mechanisms (*i.e.*, capillary action, diffusion).  
405 Overall, material thickness is a factor for increasing moisture buffering capacity [74], yet it is not a  
406 statistically significant predictor of MBV as shown in **Figure 5a**.

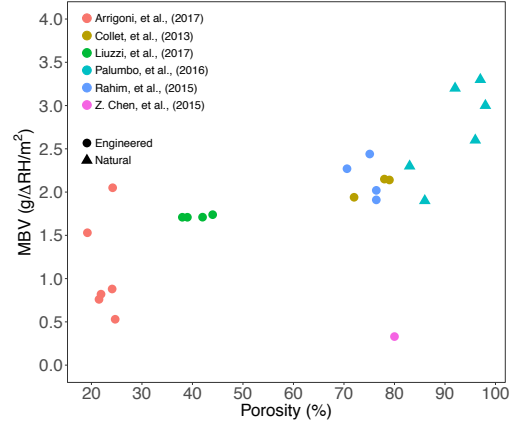
407 Porosity is an intrinsic material property that is well known to relate to the physical capacity of  
408 materials to absorb moisture [29]. As illustrated in **Figure 5b**, a more significant relationship is evident  
409 between measured sample porosity and MBV ( $R^2 = 0.46$ ). This result is expected, given that higher  
410 porosity indicates a higher propensity for water vapor to not only interact with the material (*i.e.*, increased  
411 surface area), but also potentially condense and remain in the void space. While we observed very strong

412 correlations to material densities and porosities reported in the literature (**Figure 5d**), no statistically  
413 significant relationship between density and MBV was observed (**Figure 5c**) ( $R^2 = 0.02$ ). No relationship  
414 here was expected, given that some materials, like zeolites [60] or perlite [59], may exhibit ultra-high  
415 porosities (therefore low density) and, simultaneously, a poor ability to buffer moisture. A Pearson  
416 correlation confirmed that porosity is, in fact, the only physical material property significantly correlated  
417 with MBV at a statistical significance worth considering (see **Table 4**).

418 (a)



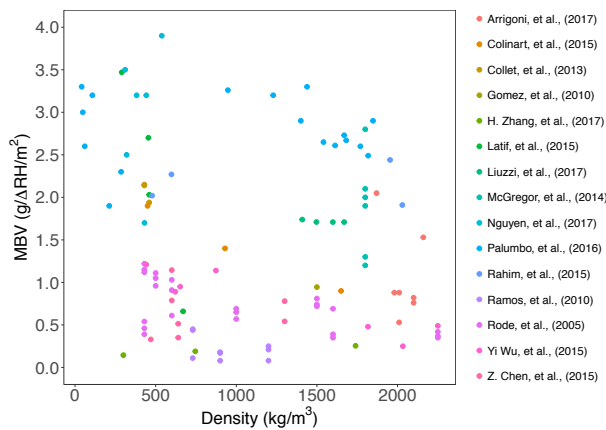
(b)



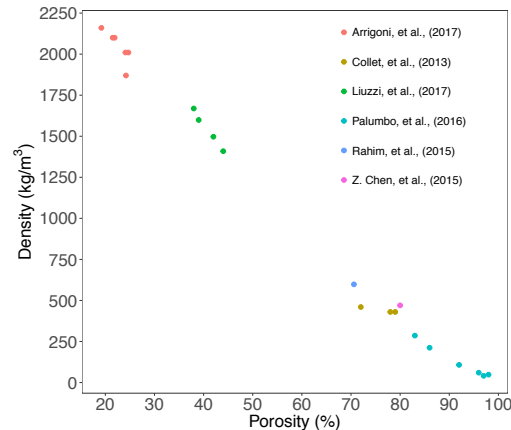
419

420

421 (c)



(d)



422

423 **Figure 5.** Reported MBV plotted versus (a) sample thickness, (b) porosity, and (c) density. Panel (d)

424 illustrates the inverse relationship between sample porosity and density.

425

426 **Table 4.** Pearson correlation values and associated statistical significance.

|           |         | MBV<br>(g/ΔRH/m <sup>2</sup> ) | Thickness<br>(mm) | Density<br>(kg/m <sup>3</sup> ) |
|-----------|---------|--------------------------------|-------------------|---------------------------------|
| Thickness | Pearson | 0.040                          | -                 | -                               |
|           | P-value | 0.738                          | -                 | -                               |
| Density   | Pearson | -0.203                         | -0.075            | -                               |
|           | P-value | 0.090                          | 0.541             | -                               |
| Porosity  | Pearson | 0.745                          | 0.512             | -0.741                          |
|           | P-value | 0.001                          | 0.051             | 0.001                           |

427

428 *2.4.4 Other Reported Properties*

429 All material characterization studies investigated in this review report other material properties that were  
430 characterized in tandem with MBV. These material properties can be grouped into two main categories:  
431 (1) intrinsic physical properties (*i.e.*, thickness, density, and porosity) or (2) RH-dependent material  
432 properties. A summary of all reported material properties—and their respective classification—are  
433 reported in **Table 5**.

434 As shown in **Figure 5**, MBV is difficult to correlate to certain intrinsic material properties (*i.e.*,  
435 thickness, density) and, as elucidated through this meta-analysis, even more difficult to correlate to the  
436 other RH-dependent material properties listed in **Table 5**. In the reviewed studies, properties that depend  
437 on RH (*e.g.*, vapor permeability, moisture diffusivity, moisture capacity) are discussed in their  
438 contribution to overall moisture buffering effect and theoretical moisture buffering values. However, we  
439 do not attempt herein to relate MBV to these other properties due to the lack of reporting and, for those  
440 that are reported, the wide variation of the RH conditions used for their characterization.

441

442



**Table 5.** Summary of hygrothermal material properties

| <i>Intrinsic Material Properties</i>    |                                    |  |
|---|------------------------------------|--|
| Property                                | Units                              | Description  |
| Sample Thickness                        | mm                                 | Material sample property generally defined by study parameters.  |
| Density                                 | kg/m <sup>3</sup>                  | Measure of compactness that directly relates to porosity and therefore available space for water sorption.   |
| Porosity                                | %                                  | Measure of voids in a material and directly related to theoretical absorption capacity of a material. The arrangement and size of these pores affect sorption and desorption mechanisms. |
| Thermal Conductivity                    | $\frac{W}{m \cdot K}$              | Ability of a material to conduct heat; changes with moisture content and is therefore RH dependent.  |
| <i>RH-Dependent Material Properties</i> |                                    |  |
| Property                                | Units                              | Description  |
| Moisture Capacity                       | $\frac{kg_{water}}{kg_{material}}$ | Capacity of water that can be held within the pore spaces of a material; determined from the slope of the sorption isotherm.   |
| Water Vapor Permeability                | $\frac{kg}{m \cdot s \cdot Pa}$    | Time- and vapor-pressure dependent value that describes the resistance of a material to transport vapor.   |
| Moisture Diffusivity                    | $\frac{m^2}{s}$                    | Rate at which moisture diffuses into a specific material; dependent on vapor pressure from ambient RH.   |
| Moisture Penetration Depth              | mm                                 | Often defined as the thickness at which the moisture content variation is only 1% that of the surface; dependent on vapor pressure from ambient RH.                                      |

444

445        These results, and those from the preceding meta-analysis, indicate that high porosity, in combination  
446 with hydrophilic chemistries of natural materials, are ideal physicochemical characteristics that lead to a  
447 high MBV. The conclusion is supported by the porosity-MBV relationship illustrated in **Figure 5b**, in  
448 which natural, highly porous materials exhibit excellent moisture buffering capacities. As explicated  
449 toward the end of this review, findings such as these have accelerated interest in capitalizing on the  
450 inherent moisture buffering properties of natural materials in the development of innovative, ultra-high  
451 moisture buffering materials and composites thereof.

452

## 453 **3.0 Review of Computational Methods**

### 454 **3.1 Modeling Methods**

#### 455 *3.1.1 Method Introduction*

456 In addition to experimental measurements, theoretical models for simulating moisture buffering and  
457 predicting their effects at the material and building scale have been formulated and implemented in the  
458 literature. These models can be classified as empirical, semi-empirical, and physics-based methods.  
459 Empirical methods are phenomenological in their exclusive use of experimental values to inform their  
460 formulation. Physics-based models, like coupled heat and moisture transfer (HAMT) models, stem from  
461 fundamental physical equations and rely on experimental data solely for validation purposes. Semi-  
462 empirical methods combine elements of both empirical and physics-based models. The classification is  
463 analogous to the more historical categorization of modeling methods as white box (empirical), grey box  
464 (semi-empirical), and black box (physics-based) approaches [75]. Ultimately, these categories help to  
465 better understand to what extent the model is being informed by experimental data or fundamentally  
466 derived equations and are helpful to consider in the validation and evaluation of these models. Due to a  
467 lack of large-scale experimental data and difficulty in even obtaining assembly- or building-scale data,  
468 recent models focus on physics-based approaches—an approach that is computationally limiting when the  
469 models are scaled in size, resolution, and complexity. We argue that, for the field to advance, a balance  
470 must be achieved between these “white box” and “black box” models to result in validated, productive  
471 simulation results for modeling the effects of moisture buffering in residential and commercial buildings.

#### 472 *3.1.2 Empirical Methods*

473 Empirical methods employed in the literature most often take simplified building models that may or may  
474 not include the moisture buffering effects of hygroscopic materials and use a correction factor, additional  
475 equations, or experimentally derived coefficients to account for an assumption that holds true in realistic  
476 and universal conditions. In effect, this approach calibrates the numerical model to represent practical  
477 MBV effects that are necessary for model validation. For example, in one study, researchers reformulated  
478 the problem to find a theoretical correction factor. The correction factor was motivated by the fact that

479 RH variations are not idealized square wave functions in realistic conditions as they are in the MBV  
480 characterization experiments [71]. The researchers model RH variation as a quasi-harmonic function and  
481 compute a correction factor and subsequent equations for moisture uptake [71]:

$$482 \quad G_{in} = G_{out} = \beta * MBV_{basic}(H - L) \quad (\text{Equation 3.1})$$

483 where  $MBV_{basic}$  is consistent with the NORDTEST ideal MBV definition and  $H$  and  $L$  are the high and  
484 low RH levels, respectively.  $G_{in}$  is moisture uptake and  $G_{out}$  as moisture release, both in  $\text{kg/m}^2$ .

485 **Equation 3.2** defines the factor  $\beta$  used in **Equation 3.1**:

$$486 \quad \beta = 0.888 * \frac{[\alpha(1-\alpha)]^{-0.035}}{\sqrt{\alpha} + \sqrt{1-\alpha}} \quad (\text{Equation 3.2})$$

487 where  $\alpha$  is a unitless time constant derived from high and low RH cycle times. After determining the  
488 correction factor, researchers tested the results against a tested and validated hygrothermal model and  
489 found good agreement (<3% relative error) [71].

490 Another strategy based solely on empirical methods is the effective capacitance model in which  
491 ambient air capacity is increased to account for the properties of hygroscopic building materials. The  
492 effective capacitance method can be within 18% error of a more advanced, computationally expensive  
493 software when it comes to component level moisture buffering effect; accurately predicting full-building  
494 RH buffering well and less-accurately predicting sudden moisture loadings [76]. Analysis of results  
495 displays an influence of hygrothermal materials on zone RH, yet little influence on overall heating and  
496 cooling demand [76]. This strategy also relies completely on the assumption that the interior space  
497 contains well-mixed air with uniform properties—an assumption that reduces computation time and  
498 simplifies the model significantly because an entire air volume of a zone can be represented as a single  
499 node where values can be extracted as averages. To improve results without losing simplicity and time,  
500 researchers coupled computational fluid dynamics (CFD) and effective penetration depth (EPD) models  
501 based on experimental data can calculate localized surface transfer coefficients for the hygric properties  
502 of simulated building walls. Adding these coefficient values to the well-mixed model successfully  
503 improved the results in cases that the surface transfer coefficient was stable and physically relevant [77].

504           In summary, the goal of the aforementioned empirical methods is to use experimental data to  
505 either create a model or improve the accuracy of a model without having to eliminate its driving  
506 assumptions. However, the primary drawback of this approach—and why it is limited in its application—  
507 is that empirical data are situational and assembly-specific, especially with a phenomenon like moisture  
508 buffering, which is highly driven by geometric factors.

### 509 3.1.3 *Semi-Empirical Methods*

510 Semi-empirical models combine physics-based and empirical methods to create a model that is rooted in  
511 derived equations and gleans additional accuracy from inputs from experimental data. Ideally, these  
512 methods also combine the efficient, *in situ*, and widespread applicability benefits of physics-based  
513 modeling with experimental data to improve accuracy and computational speed. In one example of a  
514 semi-empirical model that was employed in the literature reviewed herein, researchers used a lumped  
515 model based on effective moisture penetration depth (EMPD) that linked practical MBV to the ideal  
516 MBV as a function of moisture effusivity, RH, and air-film resistance [51]. This method uses an equation-  
517 based theory in tandem with empirical data of material properties and environmental conditions to inform  
518 the model. Using the room vapor balance and a model benchmark (discussed in further sections), the  
519 model showed between 1.5% and 50% absolute error depending on material property and material type.  
520 For practical MBV, between 7.7% and 44% absolute error was observed, depending on the material.  
521 Although large, these results performed better than the pure empirical model. Furthermore, the errors  
522 from these types models can be explained better by the quality of model inputs.

523           For determining quality inputs for a more robust semi-empirical model, an empirical method was  
524 developed by Woods *et al.* to extract data by subjecting the materials to square-wave RH profiles and,  
525 after validation, showed that the EMPD model can predict RH distributions [78]. In 2018, Woods and  
526 Winkler looked at the sensitivity of model inputs for a two-layer EMPD model for determining moisture  
527 buffering [79,80]. The two-layer model focuses on short- and long-term buffering layers and assumes  
528 cyclic RH variations, resulting in a mass-based moisture buffering determination. A sensitivity analysis  
529 showed that the deep material layer, often ignored, is an important consideration in the calculations [81].

530 However, given the difficulty of gathering data at this material layer, using the combination of  
531 experimental data-based surface inputs with physics-based equations for deep-layer moisture transport  
532 can be an efficient method for modeling hygrothermal behavior.

### 533 3.1.4 *Physics-Based Methods*

534 Physics-based methods are rooted in fundamental equations that are used to model physical phenomena.  
535 These models can quickly increase in complexity (and, therefore, computational expense) as the physical  
536 problems become more difficult (*e.g.*, coupled heat and moisture transfer). However, a comprehensive  
537 physics-based model can be easily modified to fit a variety of geometries and materials, while  
538 experimentally gathered data for empirical models are time-consuming and expensive to modify.

539 In formulating moisture uptake for numerical modeling purposes, often, Fick's law is used [82].

$$540 \quad g = -\delta_p \left( \frac{\partial p}{\partial x} \right) \quad (\text{Equation 3.3})$$

541 where moisture flux,  $g$  (kg/m<sup>2</sup>-s) is related to water vapor permeability,  $\delta_p$  [kg/m-s-Pa], and the change of  
542 water vapor pressure  $p$  [Pa] through a thickness  $x$  [mm]. As the water vapor pressure changes on the  
543 surface of the material (assuming a semi-infinite body, given that thickness is greater than theoretical  
544 moisture penetration depth), a vapor flow (moisture diffusion) is induced, and overall moisture content  
545 will increase (absorption) or decrease (desorption) over time.

546 For total moisture uptake, from which the theoretical MBV can be calculated, the moisture flux is  
547 integrated, and the water vapor permeability is replaced with  $b_m$  [kg/m<sup>2</sup>-Pa-s<sup>0.5</sup>], a term that represents  
548 surface moisture exchange:

$$549 \quad G = b_m \Delta p h(\alpha) \sqrt{\frac{t_p}{\pi}} \quad (\text{Equation 3.4})$$

550 Here,  $t_p$  is the moisture interaction time period in seconds,  $p$  is vapor pressure in Pa, and  $\alpha$  is the fraction  
551 of time period where humidity is high, so for the 8/16 hour scheme used in the NORDTEST method,  
552  $h(\alpha) = h\left(\frac{1}{3}\right) = 1.007$  because the procedure calls for *high* humidity one-third of the time. This

553 calculation results in a simplified version of the equation that is only applicable in the 8/16 hour scheme  
554 [29].

555 Drawing an analogy to heat transfer, using the moisture flux and total moisture uptake over a  
556 certain time period, the moisture effusivity of a material can be defined using a Fourier series to  
557 approximate the moisture exchange for a semi-infinite body subjected to a square wave form of moisture  
558 variation at the surface. The total moisture uptake  $G$  [kg/m<sup>2</sup>] from high to low over the time period yields  
559 the following equation that is dependent on the ratio of time the material is exposed to the *high* humidity  
560 condition [41,83].

$$561 \quad h(\alpha) \approx 2.252[\alpha(1 - \alpha)]^{0.535} \quad (\text{Equation 3.5})$$

$$562 \quad G \approx 0.568 b_m \Delta p \sqrt{t_p} \quad (\text{Equation 3.6})$$

563 Most studies recognize that, although more simplified, isolating the heat transfer and moisture  
564 transfer problems does not accurately describe the behavior of *either* phenomena due to the significant  
565 relationships between heat and moisture transport and the material properties that govern the behavior  
566 [84]. Therefore, the coupled heat, air, and moisture transfer (HAMT) strategy for hygrothermal modeling  
567 remains the prevailing, most accurate method to estimate building energy demands because it  
568 simultaneously solves equations for temperature, RH, and vapor pressure using a purely physics-based  
569 approach. A scale analysis of governing heat and moisture transfer mechanisms for hemp concrete, for  
570 example, shows that, for up to 95% RH levels, these equations are significantly coupled, and the main  
571 driver behind moisture movement in the material is the temperature gradient [85]. Above 95% RH (which  
572 is albeit unlikely to occur in a building thermal comfort context), liquid transfer and latent heat from  
573 phase changes become more significant [85]. Furthermore, a 10% increase in wood moisture content can  
574 result in 30% increases in thermal storage capacity due to the high specific heat of water [86]. However, it  
575 must be noted that heat and moisture transfer will occur on different time scales, as moisture transfer  
576 mechanisms are generally slower than heat transfer, making the computational process even more  
577 complex [86]. Overall, to be most accurate, the building energy modeling methodology must consider the

578 significantly coupled effects of heat and moisture transfer through a building envelope, as well as the  
579 timescales in which they will interact with mechanical equipment and building loads.

580         While heat flux and coupled HAMT through materials have been more extensively studied and  
581 modeled in recent years, the direction of the field continues toward eliminating simplifying assumptions  
582 to model more accurately the physical interactions in building-scale applications (*e.g.*, moisture transfer  
583 through porous media [87]). To accurately model HAMT through a building envelope and to capture the  
584 moisture buffering effect of different interior surface materials, the physical phenomena that each  
585 numerical method is modeling (and associated limitations) must be well understood. During the moisture  
586 sorption process, for example, water vapor can be transported into porous materials due to vapor pressure  
587 differentials and has the capability of condensing with the pores, then moving through the material *via*  
588 other mechanisms, such as capillary action. Condensed water also has a propensity to evaporate under  
589 certain conditions (*e.g.*, air velocity across a surface [88]). Additionally, moisture concentration and  
590 temperature do not stay uniform throughout the entire space, so surface variation and discretized time and  
591 space must be thoughtfully considered [89]. As a result, best exemplified in a numerical study of earth-  
592 based material validated with experimental data, a hygrothermal model that considers coupled HAMT,  
593 pore water pressure, and water phase changes can yield accurately model hygrothermal behavior [90].  
594 Additionally, the researchers used this validated model to evaluate the sensitivity of common modeling  
595 assumptions for earth-based material. The authors found it important to consider the impact of  
596 temperature on moisture flux and in-pore vapor mass condensation and evaporation. However, for low  
597 water permeability materials, simplifying assumptions can be made with high enough accuracy [90].

598         The last major consideration that was elucidated by this review was the importance of hysteretic  
599 effects, namely the difference in sorption and desorption isotherms, which have emerged as important  
600 sorption characteristics to consider when capturing actual hygrothermal behavior. However, only one  
601 study that was reviewed included hysteresis in the modeling methodology. Hysteretic effects (although  
602 computationally more expensive) yield better correlation to actual building-scale behavior [91].

603           When modeling the moisture buffering effect of materials in buildings, 24 hour cycles are  
604 generally needed before all components can be assumed to have reached steady-state equilibrium [91].  
605 Overall, hygrothermal models can become complex, computationally expensive, and potentially  
606 impossible to converge on a solution with user-defined acceptable relative error in this time span due to a  
607 variety of inter-related properties. In order to simplify and utilize these models, future development will  
608 need to consider the scope regarding accuracy and time-scale for the built environment, in order inform  
609 change when compared to traditional construction practices.

### 610 **3.2 Numerical Benchmarks**

611 Given the multitude of different numerical HAMT modeling approaches that have been introduced to the  
612 field in recent years, numerical benchmarks based off experimental datasets have been developed to test  
613 the accuracy of emerging software. During the IEA ECBCS Annex 41, an international collaborative  
614 project to further develop modeling of HAMT, a set of common exercises were developed to test each  
615 software [92]. Additional published test cases are available for researchers, such as the benchmark  
616 exercises from the European HAMSTAD project, to test the accuracy of their methods. These  
617 benchmarking exercises are presented in the HAMSTAD report from 2002 [93] and are used in a study by  
618 F. Tariku *et al.* [87] to validate their transient model for coupled HAMT by comparing their model results  
619 to analytical results. Judkoff and Neymark go further to recommend that three classifications of test cases  
620 should be used for model validation. These cases must include (1) an analytical verification, (2) model  
621 comparison, and (3) experimental validation [94]. In addition, Judkoff and Neymark [94] [95] have  
622 developed and continuously update [95] the NREL BESTEST base case building developed in IEA  
623 ECBCS Annex 21, which has been used to validate models from Rode *et al.* [83], Zhang *et al.* [71],  
624 Abadie *et al.* [51], Feng *et al.* [68], and software developed for the IEA Annex 41.

### 625 **3.3 Summary of Computational Methods**

626 Hygrothermal behavior is important to consider in developing more accurate building energy simulation  
627 models. Numerical simulation tools enable a relatively fast and low-cost solution to quantify building-  
628 scale benefits of materials that exhibit moisture-buffering effects and to predict and mitigate potential



629 moisture accumulation in the building envelope. For example, the ability to predict mold growth potential  
630 is an extremely valuable tool compared to costly repairs. Solutions to this particular problem are explored  
631 with WUFI-Bio [96], but the concept applies further to numerically predicting condensation in structural  
632 layers and reducing ventilation rates based off of feedback from RH sensors.

633 IEA Annex 41 explored the development of 17 different simulation tools contributed by 39  
634 institutions in 19 countries, and researchers agreed that it is necessary to model the impact of moisture to  
635 ensure accurate whole building energy simulation results [89]. The consensus made by top researchers  
636 provides further motivation for the continued development of faster, more accurate modeling tools.

637 In summary, various modeling methods categorized as *empirical*, *semi-empirical*, and *physics-*  
638 *based* have been used to model moisture buffering behavior in buildings. Each method has inherent  
639 tradeoffs in accuracy, efficiency, and expense, but progress will entail combining and refining these  
640 methods, such as coupling with CFD software to tie together material-scale and building-scale zone  
641 interactions [70] or evolutionary strategies with multi-objective searching capabilities [97]. Using  
642 advanced numerical tools in tandem with comprehensive, coupled models of HAMT, and a solid  
643 understanding of the physical processes at the building-scale and a need to verify and validate  
644 computational approaches with benchmark standards, numerical simulation remains a powerful tool that  
645 will continue to be exploited to quantify moisture buffering effects on building energy consumption.

646

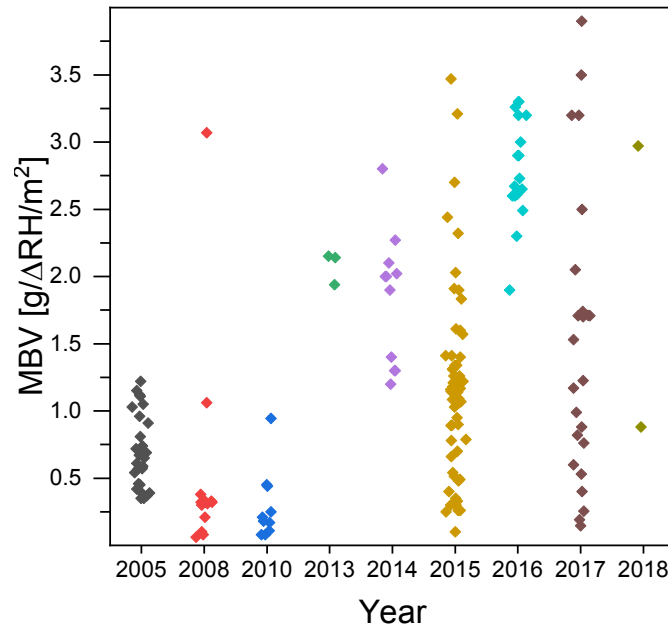
## 647 **4.0 Research Trends and Future Developments**

### 648 **4.1 Emerging and Growing Importance of MBV**

649 The results from this meta-analysis indicate not only a growing interest in understanding and  
650 characterizing moisture buffering, but also a consensus on the importance of considering moisture  
651 buffering effects in building design and operation. As illustrated in **Figure 6**, 75% of all studies that  
652 report the MBV of conventional and innovative building materials were published after 2012. The data in  
653 **Figure 6** also suggest that a wider variety of materials are being analyzed and studied with respect to their  
654 moisture buffering behavior.

655 It is anticipated that additional MBV characterization studies—especially studies that investigate the  
656 MBV of non-conventional building materials—will remain a primary interest (and need) of the field.  
657 Currently, state-of-the-art energy-efficient building design emphasizes tight, well-insulated, high-  
658 performing envelopes. The importance of ensuring indoor air quality and proper moisture management  
659 has grown in proportion to implementing energy-efficient envelope strategies. Tight envelopes reduce  
660 infiltration from outside air, frequently necessitating ventilation strategies to ensure sufficient quality of  
661 indoor air. Leveraging moisture buffering—and perhaps designing and exploiting the multifunctional  
662 potential (*e.g.*, VOC removal) of innovative, high-MBV materials—would alleviate the frequency of air  
663 exchanges in buildings. In addition, failures of these high-performance envelopes from mold or water  
664 damage are costly. Therefore, managing moisture and preventing damage due to moisture accumulation  
665 has grown in significance, especially in cold climates that require mandatory vapor retardation and where  
666 moisture swings are large due to significant heating and time spent indoors during the winter months [98].

667 Given that emerging estimates of energy savings from passive moisture buffering effects have been  
668 positive (and non-trivial), it is anticipated that accounting for moisture buffering effects in building design  
669 and operation will become more established convention. As more buildings implement building  
670 automation systems (BAS), it will be both less expensive and more feasible to include RH-sensing HVAC  
671 systems that account for the thermal conductivity and RH variations that occur within hygrothermal  
672 materials and assemblies. By combining building energy models with new, innovative materials that  
673 exhibit exceptional moisture buffering capacity, additional, passive reductions in building energy  
674 consumption could be realized. Studies with hemp-lime materials, for example, show a 5-30% cooling  
675 load reduction when using BIM to inform HVAC systems [62]. Similarly, RH-sensing ventilation systems  
676 were shown to reduce ventilation 30-40% and energy consumption 12-17% during cooling seasons [7]. In  
677 addition, full-scale wall assemblies with various building materials (*e.g.*, concrete, wood studs, hemp-  
678 lime) materials were explicitly studied to evaluate hygrothermal effects on energy consumption. Results  
679 show that these materials can potentially reduce energy use an average of 15% [4] and, depending on the  
680 climate, up to 30% [71].



681

682

**Figure 6.** Recent studies that characterize and report MBV.

683

#### 684 **4.2 Innovative Materials**

685 The results from this review indicate that best-performing hygroscopic materials for moisture buffering  
686 must exhibit high moisture uptake capacities as well as low desorption temperatures. Studies show that  
687 certain materials—especially natural materials—can exhibit over 30 times the MBV of standard building  
688 materials (*e.g.*, gypsum, plywood, concrete, plasters) [68], and this increase can impart significant savings  
689 in cost and energy to building operation when passive dehumidification through moisture buffering  
690 effects are considered. We find that most natural materials have moisture buffering effects in the *excellent*  
691 range (see **Table 6**). However, one main drawback is that their variability is higher—expectedly,  
692 engineered materials have a more statistically consistent MBV. Earth plasters with the addition of natural  
693 fibers and hempcrete mixes exhibit high moisture buffering values while not deviating to far from  
694 commonly accepted construction materials. Some more holistic, natural surface finishing products,  
695 however, such as natural wax coatings that display high MBVs, can be a cost-effective retrofit to improve  
696 the moisture buffering effects of existing buildings.

697 Novel synthetic materials, like superabsorbent hydrogels, are a promising class of materials that  
698 may be engineered to exhibit hyperactive moisture buffering behavior. Superabsorbent polymers (SAPs)  
699 are crosslinked networks of ultra-hydrophilic polymers that can absorb up to 100,000% of their dry  
700 weight in aqueous solutions [99]. The ability of the polymer to absorb fluids is attributed to the  
701 abundance of hydrophilic functional groups present on the polymer backbone, while the crosslinks in  
702 SAP networks render the polymer insoluble [100,101]. Commonplace SAPs have been synthesized using  
703 ionic acrylate/acrylamide homopolymers and biopolymers, such as alginates, celluloses, and carrageenans  
704 [102]. Theoretically, these SAPs can boost moisture buffering with much less surface area compared to  
705 other natural or synthetic materials. However, it must be noted that the ultra-high moisture affinity of  
706 SAPs may impart slower desorption, which may reduce the ability to buffer moisture when exposed to  
707 cycles of high and low RH. This phenomenon also makes some superabsorbent products, like common  
708 desiccants, non-ideal as moisture buffering materials [68].

709 As illustrated in **Table 6**, this review elucidated an increased interest in testing more innovative  
710 materials. **Table 6** lists the MBV of innovative materials and categorizes their moisture buffering  
711 behavior according to a *negligible, limited, good, and excellent* scale. New materials range from new  
712 composites made from traditional building materials (*e.g.*, clay and mortar plasters) with fiber  
713 reinforcement to highly absorbent SAP materials (*i.e.*, sodium polyacrylate). Although MIL-100, a metal  
714 organic framework, and sodium polyacrylate, a commercial SAP, do exhibit high moisture buffering  
715 values of  $15 \text{ g}/\Delta\text{RH}/\text{m}^2$  and  $9 \text{ g}/\Delta\text{RH}/\text{m}^2$  respectively, they are not yet commonly used as building  
716 materials and may not prove cost-effective or viable for achieve adequate interior surface finishes [59,68].

717 As expected, the MBVs of these new materials vary significantly. On one hand, studies of the  
718 carnauba wax particle, a natural, hydrophilic material that traps water on its rough surface, show it can  
719 boost MBV of traditional lacquered spruce board from  $0.3 \text{ g}/\Delta\text{RH}/\text{m}^2$  to  $1.1 \text{ g}/\Delta\text{RH}/\text{m}^2$  [58]. On the other  
720 hand, adding wetland phytomass in the form of typha or wool chips does not necessarily improve the  
721 MBV above the  $0.3 \text{ g}/\Delta\text{RH}/\text{m}^2$  value baseline of plain clay plaster [56], yet while adding olive fibers can

722 increase the MBV to a value of  $1.7 \text{ g}/\Delta\text{RH}/\text{m}^2$  [67]. An improvement in MBV is expected, given the  
723 moisture affinity of natural fibers, as previously discussed, but this result is not always the case.

724         In fact, **Figure 7** shows that on average, natural materials have higher moisture buffering effects  
725 ( $1.75 \text{ g}/\Delta\text{RH}/\text{m}^2$ ) than abiotic materials ( $1.075 \text{ g}/\Delta\text{RH}/\text{m}^2$ ). In distinguishing abiotic versus biotic  
726 materials; wood, organic fibers, starches, earth and clay plasters, and plant derivatives were considered  
727 biotic materials. Concretes, bricks, and gypsum, and other inorganics were considered abiotic materials,  
728 and any combination, including finish coatings (paints and lacquers) were viewed as a hybrid. With a  
729 63% increase in MBV on average when using natural, bio-based materials, exploration of more organic  
730 materials will likely be the focus of future moisture buffering studies.

731

732

733

**Table 6.** Summary of MBVs for non-conventional, innovative building materials.

734

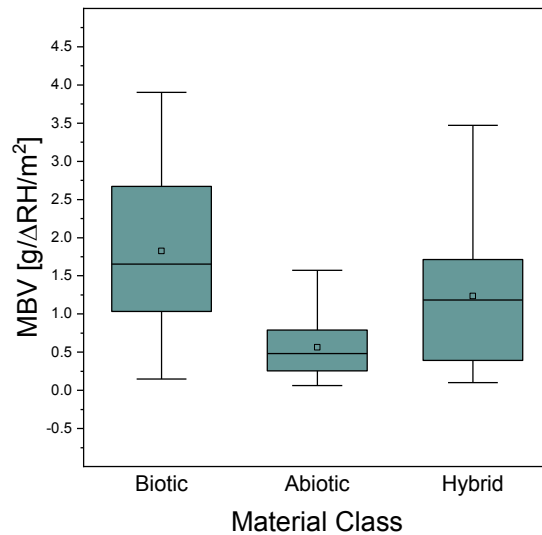
CSP = Clay, Sand, Plaster.

| Material  | MBV<br>[g/ $\Delta$ RH/m <sup>2</sup> ] | Performance<br>Category | Reference |
|---|---|-------------------------|-----------|
| CSP + 2 wt% Typha Wool                          | 0.32                                    | Limited                 | [56]      |
| CSP + 2 wt% Typha Chips                         | 0.32                                    | Limited                 | [56]      |
| CSP + 1 wt% Typha Wool and 0.5<br>wt% Chips     | 0.38                                    | Limited                 | [56]      |
| Carnauba Wax                                    | 1.085                                   | Good                    | [58]      |
| Linseed Oil                                     | 0.7                                     | Moderate                | [58]      |
| Thick Wax Film                                  | 0.1                                     | Negligible              | [58]      |
| Sodium Polyacrylate                             | 8.97                                    | Excellent               | [59]      |
| Cellulose                                       | 3.07                                    | Excellent               | [59]      |
| Bamboo Fiberboard                               | 1.7                                     | Good                    | [53]      |
| Bamboo Fiberboard (70%) and<br>Bone Glue (30%)  | 3.2                                     | Excellent               | [53]      |
| Bamboo (70%) and Sodium<br>Lignosulfonate (30%) | 3.5                                     | Excellent               | [53]      |
| Rape-Straw-Lime Concrete                        | 2.44                                    | Excellent               | [30]      |
| Flax-Lime Concrete                              | 2.27                                    | Excellent               | [30]      |
| Hemp-Lime Concrete                              | 2.02                                    | Excellent               | [30]      |
| Mortar + Date Palm Fiber                        | 2.97                                    | Excellent               | [66]      |
| Clay Plaster + Olive Fibers                     | 1.739                                   | Good                    | [67]      |
| MIL-100 (Fe)                                    | 15                                      | Excellent               | [68]      |

735

736

737



738

739 **Figure 7.** Comparison between biotic, hybrid, and abiotic material moisture buffering effects.

740

741 Given the high MBVs of biotic materials, living organisms are another emerging category of  
742 highly innovative materials that may find application in buildings as moisture buffers. While plants  
743 provide carbon dioxide (CO<sub>2</sub>) and aesthetic benefit to indoor environmental quality, plants also  
744 evapotranspire and are well known to add high humidity loads to the air [9,103–107]. Other benign living  
745 organisms, such as lichen or moss, may have a potential to serve a moisture buffering—and perhaps many  
746 other—beneficial functions to indoor environments. Such beneficial functions beyond moisture buffering  
747 could include carbon storage and sequestration, aesthetics, occupant comfort, improved indoor air quality  
748 (*e.g.*, VOC sequestration) and an ability to indicate toxic levels of environmental pollutants [108].

749 As one example, lichens possess exceptional moisture absorptive properties and abilities to  
750 sequester CO<sub>2</sub> and trap harmful pollutants. Lichen are not plants but rather a symbiotic organism  
751 comprised of fungi and algae and/or cyanobacteria. Since lichen are not plants, they do not evapotranspire  
752 nor impart excess water to the air that can increase the moisture load and contribute to more health  
753 problems and mold potential. Regarding moisture capacity, cyanobacteria-based gel lichens are able to  
754 absorb 2000% water compared to their dry weight [109,110]. These indoor water sorption properties are

755 especially useful in cold climates where increased time spent indoors leads to higher moisture loads. In  
756 addition to potential moisture sorption properties, lichens are known for their interaction with airborne  
757 pollutants. Studies show that lichen are the best accumulator of polyaromatic hydrocarbons (PAHs) that  
758 are detrimental to indoor air quality and found in high concentrations during wet winter conditions [111].  
759 Because of this, the extraction of metals and organic pollutants in lichen show that it can serve as a bio-  
760 indicator of pollutant concentrations that directly related to indoor environmental quality. Furthermore, a  
761 specific study of the species *Ramalina maciformis* also shows photosynthesis will increase with  
762 increasing water content, thereby increasing the uptake of CO<sub>2</sub> [112]. It must be noted, however, that, at a  
763 certain maximum water content, CO<sub>2</sub> uptake is inhibited, but these levels are not representative of indoor  
764 RH but of those found in heavy rain [111].

765 While true application of living materials may be more than a decade away, the majority of new  
766 materials that are emerging in the field include composite formulations of natural, hydrophilic materials,  
767 such as olive fibers, rape straw, date palm fibers, flax, and hemp, with inorganic matrices, like earthen  
768 clay plasters. However, more innovative materials, such as bamboo and wax particles, have yielded  
769 MBVs in the *excellent* range and will likely garner more attention in future studies.

770

### 771 **4.3 Advances in Building Energy Modeling**

772 In 2008, the IEA ECBCS Annex 41 identified the major problems yet to be solved in modeling heat, air,  
773 and moisture transfer [113]. The final remarks emphasized (1) establishing a balance between physical  
774 phenomena, (2) incorporating multi-dimensional and/or transient affects, and (2) using distributed  
775 calculations for computational efficiency. From 2008 to the present, advances have been made to address  
776 some of these significant problems, while some remain to be solved in relation to moisture buffering.

777 Balancing physical phenomena (*i.e.*, heat, air, and moisture) has been addressed in multiple ways by  
778 coupling software [77] and simultaneously solving heat and moisture transfer equations [90]. Coupled  
779 computational fluid dynamics (CFD) software with numerical models for solving heat and moisture  
780 transfer can now connect building elements with indoor space [113], whereas previous models made the



781 common assumption that interior spaces act as one well-mixed zone. The well-mixed zone assumption,  
782 while physically inaccurate, has been improved with CFD [77], thereby balancing physical phenomena  
783 instead of focusing specifically on building element interactions with heat and moisture.

784 Incorporating multi-dimensional and transient effects can now be considered, but these effects are not  
785 always included due to precedent and computational expense. Models can incorporate multi-dimensional  
786 heat transfer and extend heat flux to a moisture flux analogy to include multi-dimensional moisture  
787 transfer effects through building envelopes [114]. However, transient effects (*e.g.*, transient material  
788 properties, increased moisture loads in the first two years of construction) are not often considered. This  
789 current omission should be evaluated in the future for its importance, as moisture cycling is well-known  
790 to degrade materials. In addition, many other factors, like abrasion, hysteresis, and damage, can alter the  
791 time-dependent hygroscopic properties of materials that are originally included and assumed pristine in  
792 the modeling process.

793 The IEA ECBCS Annex 41 also elucidated a need for niche programs that address specialized  
794 concerns related to moisture buffering in buildings (*e.g.*, furniture-scale mold problems). This distributed  
795 calculation method would save computational time and model complexity, allowing for more advanced  
796 modeling techniques to be employed (*e.g.*, 3D heat and moisture transfer, software coupling, degradation-  
797 induced transient material properties) on a variety of scales. However, distributed modeling inputs would  
798 need to be based off full-scale modeling results to capture realistic physical phenomena—an effort that  
799 would be a significant contribution to the field.

800

## 801 **5.0 Conclusions**

802 This review highlights the materials, methods, and modeling methodologies related to the moisture  
803 buffering effect in buildings and its potential impacts on human health, indoor environmental quality,  
804 energy consumption, and occupant comfort. A multitude of materials in recent years have been  
805 characterized with respect to their moisture buffering capacities. While the most commonly employed  
806 NORDTEST method has emerged as the primary standard for materials characterization of moisture

807 buffering value (MBV), differences in experimental facilities, material heterogeneity, and operator error  
808 remain sources of measurement error for reported MBVs. Multiple sources indicate that operator error is  
809 the principal source of MBV variability. Materials-scale characterization studies of MBV are by far more  
810 common than assembly- or building-scale moisture buffering experimentation. However, results from the  
811 limited large-scale experiments and numerical studies conducted to-date report that passively controlling  
812 RH fluctuations through the moisture buffering capacities of hygroscopic materials—in a similar fashion  
813 in which thermal fluctuations are controlled with the thermal buffering effects of insulating materials—  
814 has clearly demonstrated non-trivial building energy savings potential. These findings highlight grand  
815 opportunities not only to develop and characterize novel materials with hyperactive MBVs, but also to  
816 fully understand, leverage, and quantify (*e.g.*, measure, model) the effects of moisture buffering effects at  
817 the assembly and building scale with improved accuracy.

818         More specifically, the results of this review highlight a clear, future trend in materials research,  
819 development, and characterization on porous, natural, biotic (*i.e.*, biological), and/or chemically  
820 hydrophilic (*e.g.*, superabsorbent polymers, carnauba wax) materials that exhibit high moisture buffering  
821 values (MBVs). In addition, improving the speed of HAMT modeling, while maintaining physical  
822 representativeness, will better inform building design, operation, and/or retrofit when the effects of  
823 moisture buffering are considered. These numerical models have the potential to be coupled with  
824 commercially available computational fluid dynamics software to improve assumptions and increase  
825 overall accuracy in their prediction of hygrothermal performance and energy savings potential.

826         In summary, it is evident from the literature reviewed herein that moisture buffering can yield  
827 tangible benefits by proactively considering (and designing for) the moisture buffering effects of  
828 hygroscopic materials. Future developments in materials, measurement techniques, and modeling  
829 approaches will only maximize the benefits of moisture buffering to reduce building energy consumption  
830 and further improve indoor environmental quality.

831

832

833 **6.0 Acknowledgments**

834 This research was made possible by the Department of Civil, Environmental, and Architectural  
835 Engineering and the Living Materials Laboratory (LMLab) at the University of Colorado Boulder with  
836 financial support from the College of Engineering and Applied Sciences Multifunctional Materials  
837 Interdisciplinary Research Theme (IRT) Seed Grant Program. This work represents the views of the  
838 authors and not necessarily those of the sponsors.

839

840 **7.0 References**

- 841 [1] U.S. Energy Information Administration, Annual Energy Review, 2017.  
842 <https://www.eia.gov/totalenergy/data/annual/index.php>.
- 843 [2] Office of Energy Efficiency & Renewable Energy, HVAC, Water Heating, and Appliances, 2018.  
844 <https://www.energy.gov/eere/buildings/hvac-water-heating-and-appliances>.
- 845 [3] N. Mendes, F.C. Winkelmann, R. Lamberts, P.C. Philippi, Moisture effects on conduction loads,  
846 35 (2003) 631–644.
- 847 [4] A.S. Nordby, A.D. Shea, Building Materials in the Operational Phase Impacts of Direct Carbon  
848 Exchanges and Hygrothermal Effects, 17 (2013) 763–776. doi:10.1111/jiec.12046.
- 849 [5] O.F. Osanyintola, C.J. Simonson, Moisture buffering capacity of hygroscopic building materials:  
850 Experimental facilities and energy impact, Energy Build. 38 (2006) 1270–1282.  
851 doi:10.1016/j.enbuild.2006.03.026.
- 852 [6] O. Adan, H. Brocken, J. Carmeliet, H. Hens, S. Roels, C.-E. Hagentoft, Determination of Liquid  
853 Water Transfer Properties of Porous Building Materials and Development of Numerical  
854 Assessment Methods : Introduction to the EC HAMSTAD Project, J. Therm. Env. Bldg. Sci. 27  
855 (2004) 253–260. doi:10.1177/1097196304042323.
- 856 [7] M. Woloszyn, T. Kalamees, M. Olivier, M. Steeman, A. Sasic, The effect of combining a relative-  
857 humidity-sensitive ventilation system with the moisture-buffering capacity of materials on indoor  
858 climate and energy efficiency of buildings, 44 (2009) 515–524.

- 859           doi:10.1016/j.buildenv.2008.04.017.
- 860 [8]   T. Lu, X. Lu, M. Viljanen, Moisture and Estimation of Moisture Generation Rate, *Intech. 2* (2018)
- 861           25. doi:10.5772/32009.
- 862 [9]   J. Christian, *Moisture Control in Buildings: The Key Factor in Mold Prevention*, 1st ed., American
- 863           Society for Testing and Materials, Philadelphia, 1994.
- 864 [10]   Lieff, R. Trechsel, *Moisture Migration in Buildings*, 1st ed., American Society for Testing and
- 865           Materials, Philadelphia, 1982.
- 866 [11]   D. Erhardt, M. Mecklenburg, Relative humidity re-examined, *Stud. Conserv. 39* (1994) 32–38.
- 867           doi:10.1179/sic.1994.39.Supplement-2.32.
- 868 [12]   Q. Wu, C. Piao, Thickness Swelling and its Relationship to Internal Bond Strength Loss of
- 869           Commercial Oriented Strandboard, *For. Prod. J. 49* (1999) 50.
- 870 [13]   American Wood Council, *National Design Specification for Wood Construction - 2018*, Leesburg,
- 871           VA, 2018.
- 872 [14]   S. Jacobsen, E.J. Sellevold, SELF HEALING OF HIGH STRENGTH CONCRETE AFTER
- 873           DETERIORATION BY FREEZE / THAW, *Cem. Concr. Res. 26* (1996) 55–62.
- 874 [15]   P.L. Gaspar, J. De Brito, Quantifying environmental effects on cement-rendered facades : A
- 875           comparison between different degradation indicators, *Build. and Environ. 43* (2008) 1818–1828.
- 876           doi:10.1016/j.buildenv.2007.10.022.
- 877 [16]   N. Lucas, C. Bienaime, C. Belloy, M. Queneudec, F. Silvestre, J. Nava-saucedo, Polymer
- 878           biodegradation : Mechanisms and estimation techniques, *Chemosphere. 73* (2008) 429–442.
- 879           doi:10.1016/j.chemosphere.2008.06.064.
- 880 [17]   F. Debieb, L. Courard, S. Kenai, R. Degeimbre, Mechanical and durability properties of concrete
- 881           using contaminated recycled aggregates, *Cem. Concr. Compos. 32* (2010) 421–426.
- 882           doi:10.1016/j.cemconcomp.2010.03.004.
- 883 [18]   W. Srubar, An analytical model for predicting the freeze-thaw durability of wood-fiber
- 884           composites, *Compos. Part B Eng. 69* (2015) 435–442. doi:10.1016/j.compositesb.2014.10.1015.

- 885 [19] H. Viitanen, J. Vinha, K. Salminen, T. OJanen, R. Peuhkuri, L. Paajanen, K. Lahdesmaki,  
886 Moisture and Bio-deterioration Risk of Building Materials and Structures, *J. Build. Phys.* 33  
887 (2010). doi:10.1177/1744259109343511.
- 888 [20] S. Klaus, M. Krus, K. Breuer, MOULD GROWTH PREDICTION WITH A NEW  
889 BIOHYGROTHERMAL METHOD AND ITS APPLICATION IN PRACTICE, Holzkirchen,  
890 2001.
- 891 [21] J.Y. Bergen, *House Air*, *Science* (80-. ). 34 (1911) 407–408.
- 892 [22] W. Kent, W. Crowell, L. Jones, *The Air We Breathe*, *Science* (80-. ). 33 (1911) 486–491.
- 893 [23] L.R. Ingersoll, *Indoor Air*, *Science* (80-. ). XXXVII (1913) 524–525.
- 894 [24] L.M. Reinikainen, J.J.K. Jaakkola, Significance of humidity and temperature on skin and upper  
895 airway symptoms, *Indoor Air*. 13 (2003) 344–352.
- 896 [25] C.G. Bornehag, J. Sundell, S. Bonini, A. Custovic, P. Malmberg, S. Skerfving, T. Sigsgaard, A.  
897 Verhoeff, Dampness in buildings as a risk factor for health effects , *EUROEXPO : a*  
898 *multidisciplinary review of the literature ( 1998 – 2000 ) on dampness and mite exposure in*  
899 *buildings and health effects*, *Indoor Air*. 14 (2004) 243–257. doi:10.1111/j.1600-  
900 0668.2004.00240.x.
- 901 [26] ASHRAE, ANSI/ASHRAE Standard 62.1 - 2013, Atlanta, GA, 2013.
- 902 [27] A. Datta, R. Suresh, A. Gupta, D. Singh, P. Kulshrestha, Indoor air quality of non-residential  
903 urban buildings in Delhi , India, *Int. J. Sustain. Built Environ.* 6 (2017) 412–420.  
904 doi:10.1016/j.ijsbe.2017.07.005.
- 905 [28] S. Jing, B. Li, M. Tan, H. Liu, Impact of Relative Humidity on Thermal Comfort in a Warm  
906 Environment, *Indoor Built Environ.* 22 (2012) 598–607. doi:10.1177/1420326X12447614.
- 907 [29] C. Rode, R. Peuhkuri, L.H. Mortensen, K.K. Hansen, A. Gustavsen, T. Ojanen, J. Ahonen, K.  
908 Svennberg, L.-E. Harderup, J. Arfvidsson, *Moisture Buffering of Building Materials*, Nordisk  
909 Innovations Center, 2005.  
910 [http://orbit.dtu.dk/fedora/objects/orbit:75984/datastreams/file\\_2415500/content](http://orbit.dtu.dk/fedora/objects/orbit:75984/datastreams/file_2415500/content).

- 911 [30] M. Rahim, O. Douzane, A.D.T. Le, G. Promis, B. Laidoudi, A. Crigny, B. Dupre, T. Langlet,  
912 Characterization of flax lime and hemp lime concretes : Hygric properties and moisture buffer  
913 capacity, *Energy Build.* 88 (2015) 91–99. doi:10.1016/j.enbuild.2014.11.043.
- 914 [31] K. Svennberg, K. Lengsfeld, Previous Experimental Studies and Field Measurements on Moisture  
915 Buffering by Indoor Surface Materials, *J. Build. Phys.* 30 (2007).  
916 doi:10.1177/1744259107073221.
- 917 [32] T. Padfield, L.A. Jensen, Humidity buffering by absorbent materials, (2010) 1–11.
- 918 [33] JIS (Japanese Industrial Standard), A1470: Test method of adsorption/desorption efficiency for  
919 building materials to regulate an indoor humidity - part 1: response method of humidity, JIS,  
920 Tokyo, Japan, 2002.
- 921 [34] ISO (International Standards Organization), ISO 24353: Hygrothermal performance of building  
922 materials and products - determination of moisture adsorption/desorption properties in response to  
923 humidity variation., ISO, Geneva, Switzerland, 2008.
- 924 [35] DIN (Deutsches Institut für Normung), No DIN 18947:2013-08: Earth plasters - terms and  
925 definitions, requirements, test methods, NABau, Berlin, Germany, 2013.
- 926 [36] H. Kunzel, Die Feuchtigkeitsabsorption von Innenoberflächen und Inneneinrichtungen, *Berichte*  
927 *Aus Der Bauforsch.* (1965) 102–116.
- 928 [37] J. Lima, P. Faria, Eco-efficient earthen plasters: The influence of the addition of natural fibers,  
929 *RILEM Bookseries.* 12 (2016) 315–327. doi:10.1007/978-94-017-7515-1\_24.
- 930 [38] F. McGregor, A. Heath, D. Maskell, A. Fabbri, J. Morel, A review on the buffering capacity of  
931 earth building materials, *Constr. Mater.* 169 (2016).
- 932 [39] S. Roels, H. Janssen, A Comparison of the Nordtest and Moisture Buffering Performance, *J. Build.*  
933 *Phys.* 30 (2006). doi:10.1177/1744259106068101.
- 934 [40] M. Rahim, O. Douzane, A.D.T. Le, G. Promis, T. Langlet, Characterization and comparison of  
935 hygric properties of rape straw concrete and hemp concrete, 102 (2016) 679–687.  
936 doi:10.1016/j.conbuildmat.2015.11.021.

- 937 [41] R. Peuhkuri, C. Rode, Moisture buffer value: Analytical determination and use of dynamic  
938 measurements, 2005.
- 939 [42] I. Gómez, S. Guths, R. Souza, J.A. Millan, K. Martín, J.M. Sala, Moisture buffering performance  
940 of a new pozolanic ceramic material: Influence of the film layer resistance, *Energy Build.* 43  
941 (2011) 873–878. doi:10.1016/j.enbuild.2010.12.007.
- 942 [43] Y. Wu, G. Gong, C. Wah, Z. Huang, Proposing ultimate moisture buffering value ( UMBV ) for  
943 characterization of composite porous mortars, 82 (2015) 81–88.  
944 doi:10.1016/j.conbuildmat.2015.02.058.
- 945 [44] J. Kurnitski, T. Kalamees, J. Palonen, L. Eskola, O. Seppanen, Potential effects of permeable and  
946 hygroscopic lightweight structures on thermal comfort and perceived IAQ in a cold climate,  
947 *Indoor Air.* (2007) 37–49. doi:10.1111/j.1600-0668.2006.00447.x.
- 948 [45] A. Holm, K. Lengsfeld, Moisture-Buffering Effect — Experimental Investigations and Validation,  
949 (2007).
- 950 [46] C.J. Simonson, M. Salonvaara, T. Ojanen, Indoor Air and a Permeable and Hygroscopic Building  
951 Envelope :, *J. Build. Phys.* 28 (n.d.). doi:10.1177/1097196304044395.
- 952 [47] L. Shi, H. Zhang, Z. Li, X. Man, Y. Wu, C. Zheng, J. Liu, Analysis of moisture buffering effect of  
953 straw-based board in civil defence shelters by field measurements and numerical simulations,  
954 *Build. Environ.* 143 (2018) 366–377. doi:10.1016/j.buildenv.2018.07.018.
- 955 [48] H. Zhang, H. Yoshino, K. Hasegawa, J. Liu, W. Zhang, H. Xuan, Practical moisture buffering  
956 effect of three hygroscopic materials in real-world conditions, *Energy Build.* 139 (2017) 214–223.  
957 doi:10.1016/j.enbuild.2017.01.021.
- 958 [49] H.J. Moon, S.H. Ryu, J.T. Kim, The effect of moisture transportation on energy efficiency and  
959 IAQ in residential buildings, *Energy Build.* 75 (2014) 439–446.  
960 doi:10.1016/j.enbuild.2014.02.039.
- 961 [50] W. V Srubar, C.W. Frank, S.L. Billington, Modeling the kinetics of water transport and  
962 hydroexpansion in a lignocellulose-reinforced bacterial copolyester, *Polymer (Guildf).* 53 (2012)

- 963 2152–2161. doi:10.1016/j.polymer.2012.03.036.
- 964 [51] M.O. Abadie, K.C. Mendonça, Moisture performance of building materials: From material  
965 characterization to building simulation using the Moisture Buffer Value concept, *Build. Environ.*  
966 44 (2009) 388–401. doi:10.1016/j.buildenv.2008.03.015.
- 967 [52] T. Colinart, D. Lelievre, P. Glouannec, Experimental and numerical analysis of the transient  
968 hygrothermal behavior of multilayered hemp concrete wall, *Energy Build.* 112 (2016) 1–11.  
969 doi:10.1016/j.enbuild.2015.11.027.
- 970 [53] D.M. Nguyen, A.C. Grillet, T.M.H. Diep, C.N. Ha Thuc, M. Woloszyn, Hygrothermal properties  
971 of bio-insulation building materials based on bamboo fibers and bio-glues, *Constr. Build. Mater.*  
972 155 (2017) 852–866. doi:10.1016/j.conbuildmat.2017.08.075.
- 973 [54] N.M.M. Ramos, J.M.P.Q. Delgado, V.P. De Freitas, Influence of finishing coatings on  
974 hygroscopic moisture buffering in building elements, *Constr. Build. Mater.* 24 (2010) 2590–2597.  
975 doi:10.1016/j.conbuildmat.2010.05.017.
- 976 [55] M. Palumbo, F. McGregor, A. Heath, P. Walker, The influence of two crop by-products on the  
977 hygrothermal properties of earth plasters, *Build. Environ.* 105 (2016) 245–252.  
978 doi:10.1016/j.buildenv.2016.06.004.
- 979 [56] M. Maddison, T. Mairing, K. Kirsimäe, Ü. Mander, The humidity buffer capacity of clay-sand  
980 plaster filled with phytomass from treatment wetlands, *Build. Environ.* 44 (2009) 1864–1868.  
981 doi:10.1016/j.buildenv.2008.12.008.
- 982 [57] A. Arrigoni, A.C. Grillet, R. Pelosato, G. Dotelli, C.T.S. Beckett, M. Woloszyn, D. Ciancio,  
983 Reduction of rammed earth’s hygroscopic performance under stabilisation: an experimental  
984 investigation, *Build. Environ.* 115 (2017) 358–367. doi:10.1016/j.buildenv.2017.01.034.
- 985 [58] A. Lozhechnikova, K. Vahtikari, M. Hughes, M. Österberg, Toward energy efficiency through an  
986 optimized use of wood: The development of natural hydrophobic coatings that retain moisture-  
987 buffering ability, *Energy Build.* 105 (2015) 37–42. doi:10.1016/j.enbuild.2015.07.052.
- 988 [59] S. Cerolini, M. D’Orazio, C. Di Perna, A. Stazi, Moisture buffering capacity of highly absorbing



- 989 materials, *Energy Build.* 41 (2009) 164–168. doi:10.1016/j.enbuild.2008.08.006.
- 990 [60] Z. Chen, M. Qin, Preparation and hygrothermal properties of composite phase change humidity  
991 control materials, *Appl. Therm. Eng.* 98 (2016) 1150–1157.  
992 doi:10.1016/j.applthermaleng.2015.12.096.
- 993 [61] Z. Chen, M. Qin, J. Yang, Synthesis and characteristics of hygroscopic phase change material:  
994 Composite microencapsulated phase change material (MPCM) and diatomite, *Energy Build.* 106  
995 (2015) 175–182. doi:10.1016/j.enbuild.2015.05.033.
- 996 [62] E. Latif, M. Lawrence, A. Shea, P. Walker, Moisture buffer potential of experimental wall  
997 assemblies incorporating formulated hemp-lime, *Build. Environ.* 93 (2015) 199–209.  
998 doi:10.1016/j.buildenv.2015.07.011.
- 999 [63] F. McGregor, A. Heath, A. Shea, M. Lawrence, The moisture buffering capacity of un fi red clay  
1000 masonry, *Build. Environ.* 82 (2014) 599–607. doi:10.1016/j.buildenv.2014.09.027.
- 1001 [64] F. Collet, J. Chamoin, S. Pretot, C. Lanos, Comparison of the hygric behaviour of three hemp  
1002 concretes, *Energy Build.* 62 (2013) 294–303. doi:10.1016/j.enbuild.2013.03.010.
- 1003 [65] M. Palumbo, A.M. Lacasta, N. Holcroft, A. Shea, P. Walker, Determination of hygrothermal  
1004 parameters of experimental and commercial bio-based insulation materials, *Constr. Build. Mater.*  
1005 124 (2016) 269–275. doi:10.1016/j.conbuildmat.2016.07.106.
- 1006 [66] N. Chennouf, B. Agoudjil, A. Boudenne, Hygrothermal Study of Mortar with Date Palm Fiber  
1007 Reinforcement, 020013 (2018). doi:10.1063/1.5047607.
- 1008 [67] S. Liuzzi, C. Rubino, P. Stefanizzi, A. Petrella, A. Boghetich, C. Casavola, G. Pappaletta,  
1009 Hygrothermal properties of clayey plasters with olive fibers, *Constr. Build. Mater.* 158 (2018) 24–  
1010 32. doi:10.1016/j.conbuildmat.2017.10.013.
- 1011 [68] X. Feng, M. Qin, S. Cui, C. Rode, Metal-organic framework MIL-100 ( Fe ) as a novel moisture  
1012 bu ff er material for energy-e ffi cient indoor humidity control, *Build. Environ.* 145 (2018) 234–  
1013 242. doi:10.1016/j.buildenv.2018.09.027.
- 1014 [69] A. Arrigoni, C.T.S. Beckett, D. Ciancio, R. Pelosato, G. Dotelli, A. Grillet, Resources ,

- 1015 Conservation & Recycling Rammed Earth incorporating Recycled Concrete Aggregate : a  
1016 sustainable , resistant and breathable construction solution, *Resour. Conserv. Recycl.* 137 (2018)  
1017 11–20. doi:10.1016/j.resconrec.2018.05.025.
- 1018 [70] H. Zhang, H. Yoshino, A. Iwamae, K. Hasegawa, Investigating simultaneous transport of heat and  
1019 moisture in hygroscopic materials by a semi-conjugate CFD-coupled approach, *Build. Environ.* 90  
1020 (2015) 125–135. doi:10.1016/j.buildenv.2015.03.028.
- 1021 [71] M. Zhang, M. Qin, C. Rode, Z. Chen, Moisture buffering phenomenon and its impact on building  
1022 energy consumption, *Appl. Therm. Eng.* 124 (2017) 337–345.  
1023 doi:10.1016/j.applthermaleng.2017.05.173.
- 1024 [72] C. Feng, H. Janssen, Y. Feng, Q. Meng, Hygric properties of porous building materials : Analysis  
1025 of measurement repeatability and reproducibility, *Build. Environ.* 85 (2015) 160–172.  
1026 doi:10.1016/j.buildenv.2014.11.036.
- 1027 [73] S. Roels, P. Talukdar, C. James, C.J. Simonson, Reliability of material data measurements for  
1028 hygroscopic buffering, *Int. J. Heat Mass Transf.* 53 (2010) 5355–5363.  
1029 doi:10.1016/j.ijheatmasstransfer.2010.07.020.
- 1030 [74] D. Maskell, A. Thomson, P. Walker, M. Lemke, Determination of optimal plaster thickness for  
1031 moisture buffering of indoor air, *Build. Environ.* 130 (2018) 143–150.  
1032 doi:10.1016/j.buildenv.2017.11.045.
- 1033 [75] R. Kramer, J. van Schijndel, H. Schellen, Simplified thermal and hygric building models: A  
1034 literature review, *Front. Archit. Res.* 1 (2012) 318–325. doi:10.1016/j.foar.2012.09.001.
- 1035 [76] M. Barclay, N. Holcroft, A.D. Shea, Methods to determine whole building hygrothermal  
1036 performance of hemp-lime buildings, *Build. Environ.* 80 (2014) 204–212.  
1037 doi:10.1016/j.buildenv.2014.06.003.
- 1038 [77] H.J. Steeman, A. Janssens, J. Carmeliet, M. De Paepe, Modelling indoor air and hygrothermal wall  
1039 interaction in building simulation : Comparison between CFD and a well-mixed zonal model, 44  
1040 (2009) 572–583. doi:10.1016/j.buildenv.2008.05.002.

- 1041 [78] J. Woods, J. Winkler, Field measurement of moisture-buffering model inputs for residential  
1042 buildings, *Energy Build.* 117 (2016) 91–98. doi:10.1016/j.enbuild.2016.02.008.
- 1043 [79] J. Woods, J. Winkler, Effective moisture penetration depth model for residential buildings:  
1044 Sensitivity analysis and guidance on model inputs, *Energy Build.* 165 (2018) 216–232.  
1045 doi:10.1016/j.enbuild.2018.01.040.
- 1046 [80] J. Woods, J. Winkler, D. Christensen, Moisture modeling: Effective moisture penetration depth  
1047 versus effective capacitance, in: *Proc. Int. Conf. Therm. Perform. Exter. Envel. Whole Build. XII*,  
1048 Clearwater, FL, 2013: pp. 216–232.
- 1049 [81] J. Woods, J. Winkler, D. Christensen, Evaluation of the effective moisture penetration depth  
1050 (EMPD) model for estimating moisture buffering in buildings, 2013.
- 1051 [82] H. Kunzel, I. Habil, K. Gertis, *Simultaneous Heat and Moisture Transport In Building*  
1052 *Components*, 1995.
- 1053 [83] C. Rode, K. Grau, Moisture buffering and its consequence in whole building hygrothermal  
1054 modeling, *J. Build. Phys.* 31 (2008) 333–360. doi:10.1177/1744259108088960.
- 1055 [84] H. Kuenzel, A. Karagiozis, A. Holm, A Hygrothermal design tool for architects and engineers, in:  
1056 *Moisture Analysis and Condensation Control in Building Envelopes*, in: *ASTM Man. Ser. 50*,  
1057 2001.
- 1058 [85] B. Seng, S. Lorente, C. Magniont, Scale analysis of heat and moisture transfer through bio-based  
1059 materials — Application to hemp concrete, *Energy Build.* 155 (2017) 546–558.  
1060 doi:10.1016/j.enbuild.2017.09.026.
- 1061 [86] S. Hameury, Moisture buffering capacity of heavy timber structures directly exposed to an indoor  
1062 climate: A numerical study, *Build. Environ.* 40 (2005) 1400–1412.  
1063 doi:10.1016/j.buildenv.2004.10.017.
- 1064 [87] F. Tariku, K. Kumaran, P. Fazio, *International Journal of Heat and Mass Transfer* Transient model  
1065 for coupled heat , air and moisture transfer through multilayered porous media, *Int. J. Heat Mass*  
1066 *Transf.* 53 (2010) 3035–3044. doi:10.1016/j.ijheatmasstransfer.2010.03.024.

- 1067 [88] P. Plathner, M. Woloszyn, Interzonal air and moisture transport in a test house : experiment and  
1068 modelling, 37 (2002) 189–199.
- 1069 [89] M. Woloszyn, C. Rode, Tools for Performance Simulation of Heat , Air and Moisture Conditions  
1070 of Whole Buildings, (2008) 5–24. doi:10.1007/s12273-008-8106-z.
- 1071 [90] L. Soudani, A. Fabbri, J. Morel, M. Woloszyn, P. Chabriac, H. Wong, A. Grillet, Assessment of  
1072 the validity of some common assumptions in hygrothermal modeling of earth based materials,  
1073 Energy Build. 116 (2016) 498–511. doi:10.1016/j.enbuild.2016.01.025.
- 1074 [91] G. Promis, O. Douzane, A.D. Tran Le, T. Langlet, Moisture hysteresis influence on mass transfer  
1075 through bio-based building materials in dynamic state, Energy Build. 166 (2018) 450–459.  
1076 doi:10.1016/j.enbuild.2018.01.067.
- 1077 [92] M. Woloszyn, C. Rode, Subtask 1 - Modelling Principles and Common Exercises, 2007.
- 1078 [93] C.-E. Hagentoft, HAMSTAD - Final report: methodology of HAM-modeling, Report R-02:8,  
1079 Gothenburg, 2002.
- 1080 [94] R. Judkoff, J. Neymark, Building energy simulation test (BESTEST) and diagnostic method,  
1081 NREL/TP-472-6231, Golden, CO, 1995.
- 1082 [95] R. Judkoff, J. Neymark, Twenty Years On!: Updating the IEA BESTEST Building Thermal Fabric  
1083 Test Cases for ASHRAE Standard 140 NREL/CP - 5500-58487, Chambéry, France, 2013.
- 1084 [96] K. Holzhueter, K. Itonaga, An Evaluation of WUFI-Bio to Predict Mold Growth in Straw Bale  
1085 Walls in Japan, (2017) 357–362.
- 1086 [97] S. Rouchier, M. Woloszyn, Y. Kedowide, T. Béjat, Identification of the hygrothermal properties of  
1087 a building envelope material by the covariance matrix adaptation evolution strategy, 1493 (2016).  
1088 doi:10.1080/19401493.2014.996608.
- 1089 [98] ICC (International Code Council), Residential Energy Efficiency, in: 2018 IECC (International  
1090 Energy Conserv. Code), ICC, Washington, DC, 2018.
- 1091 [99] M.J. Zohuriaan-Mehr, K. Kabiri, Superabsorbent Polymer Materials, Iran. Polym. J. (2008) 451–  
1092 477. doi:doi:http://journal.ippi.ac.ir.

- 1093 [100] E.M. Ahmed, Hydrogel: Preparation, characterization, and applications: A review, *J. Adv. Res.* 6  
1094 (2015) 105–121. doi:10.1016/j.jare.2013.07.006.
- 1095 [101] F.L. Buchholz, A.T. Graham, *Modern Superabsorbent Polymer Technology*, Wiley-VCH, 1998.
- 1096 [102] E. Feng, G. Ma, Y. Wu, H. Wang, Z. Lei, Preparation and properties of organic-inorganic  
1097 composite superabsorbent based on xanthan gum and loess, *Carbohydr. Polym.* 111 (2014) 463–  
1098 468. doi:10.1016/j.carbpol.2014.04.031.
- 1099 [103] T. Kalamees, J. Vinha, J. Kurnitski, Indoor Humidity Loads and Moisture Production in  
1100 Lightweight Timber-frame Detached Houses, *J. Build. Phys.* 29 (2006) 219–246.  
1101 doi:10.1177/1744259106060439.
- 1102 [104] W.J. Angell, *Home Moisture Sources*, CD-FS. (1988).
- 1103 [105] CIBSE, *Gude A: Environmental Design*, 1999.
- 1104 [106] A.P. Koch, *Fugt i boligen*, 1986.
- 1105 [107] BS 5250, *British Standard Code of Practice for Control of Condensation in Buildings*, 1989.
- 1106 [108] R.M. Easton, *Lichens and Rocks: A Review*, *Geosci. Canada.* 21 (1995).
- 1107 [109] Y. Gauslaa, Rain , dew , and humid air as drivers of morphology , function and spatial distribution  
1108 in epiphytic lichens, 46 (2018) 1–16. doi:10.1017/S0024282913000753.
- 1109 [110] P.-A. Esseen, M. Ronnqvist, Y. Gauslaa, D.S. Coxson, Externally held water - a key factor for hair  
1110 lichens in boreal forest canopies, *Fungal Ecol.* 30 (2017) 29–38.  
1111 doi:10.1016/j.funeco.2017.08.003.
- 1112 [111] L. Van der Wat, P.B.C. Forbes, Lichens as biomonitors for organic air pollutants, *TrAC - Trends*  
1113 *Anal. Chem.* 64 (2015) 165–172. doi:10.1016/j.trac.2014.09.006.
- 1114 [112] O.L. Lange, J.D. Tenhunen, Moisture content and CO<sub>2</sub>exchange of lichens. II. Depression of net  
1115 photosynthesis in *Ramalina maciformis* at high water content is caused by increased thallus carbon  
1116 dioxide diffusion resistance, *Oecologia.* 51 (1981) 426–429. doi:10.1007/BF00540917.
- 1117 [113] A. Janssens, M. Woloszyn, C. Rode, A. Sasic-Kalagasidis, M. De Paepe, From EMPD to CFD –  
1118 overview of different approaches for Heat Air and Moisture modeling in IEA Annex 41, in: *Proc.*

Manuscript submitted to:  
*Energy and Buildings*

1119 IEA ECBCS Annex 41 Closing Semin., Copenhagen, Denmark, 2008.

1120 [114] F.I.F.B. Physics, WUFI Plus, (2019) 4.

1121